Analyzing Gravure Cylinder Engraving Factors to Reduce White Ink Consumption and Improve Spot Color Quality on clear CPET Films

Kanishka Sahu

Abstract

Gravure printing on transparent substrates, such as clear CPET films, requires a white ink underlay to achieve vibrant spot color reproduction and opacity. White ink underlays play a critical role in reverse gravure printing on transparent substrates by enhancing color vibrancy, suppressing background interference, and ensuring consistent spot color reproduction. These underlayers act as an optical barrier, enhancing opacity, suppressing background interference, and enabling accurate color rendering in reverse-printed packaging applications (Eller & D'Amico, 2022; Tomerlin et al., 2023). However, white ink is also one of the most resource-intensive inks used in packaging, making its optimization crucial for cost efficiency and sustainability (Desai & Hansen, n.d.). While previous studies have explored ink transfer characteristics and print quality at a broad level (Gencoglu, 2005; Deng et al., 2014), there remains a lack of systematic, quantitative investigations linking specific gravure engraving parameters to white ink consumption and spot color accuracy on transparent films.

This study investigates the effects of gravure engraving parameters: line screen, screen angle, and stylus angle, on white ink consumption, opacity, lightness (L*), and ΔE00 spot color accuracy when printing on 45-micron clear Crystallized Polyethylene Terephthalate (CPET) film. Both single-hit and two-hit white underlay configurations were evaluated under varying ink viscosities, with print performance metrics collected and analyzed through correlation analysis, ANOVA, and regression modeling. Results revealed a strong positive correlation between engraving cell volume in Billion Cubic Microns (BCM) and both opacity and lightness, validating the critical role of ink volume in achieving optimal visual outcomes.

However, variations in ΔE00 for spot colors were partially explained by BCM,

Rochester Institute of Technology, Rochester, NY

indicating that additional variables influence spot color fidelity.

An optimization study using JMP's Prediction Profiler, identified 33 engraving combinations capable of reducing total white ink laydown below the industry-standard engraving combination with cell volume of 20.8 BCM while maintaining acceptable print quality and color fidelity. These findings support the application of data-driven optimization in gravure printing to reduce ink consumption without compromising print quality, while also highlighting areas for future research in color variability and ink-substrate interactions.

Introduction

White ink underlayers play an essential role in gravure and flexographic printing, particularly for achieving vibrant and consistent spot color reproduction on transparent substrates such as Crystallized Polyethylene Terephthalate (CPET) films. These underlayers act as an optical barrier, enhancing opacity, suppressing background interference, and enabling accurate color rendering in reverse-printed packaging applications (Eller & D'Amico, 2022; Tomerlin et al., 2023). However, white ink is also one of the most resource-intensive inks in the printing process, often comprising 40–50% of total ink consumption (Desai & Hansen, n.d.). This makes the optimization of white ink usage a significant lever for cost reduction and sustainability improvement in high-volume packaging production.

Gravure printing, as an intaglio method, utilizes engraved cylinders that transfer ink through micro-etched cells. Key parameters such as line screen, screen angle, and stylus angle determine the geometry and volume of these cells, directly influencing ink laydown, transfer efficiency, and final visual appearance (Ozcan & Zulfigaroglu, 2020; Neff, 2009). Similarly, in flexography, anilox rollers serve a functionally analogous role: metering and delivering controlled volumes of ink to the printing plate. Just like gravure cylinders, anilox rollers rely on engraved cells, and their performance depends on key geometric parameters such as cell volume, line screen, and cell angle. The volume of ink carried is especially sensitive to the engraving geometry, and minor discrepancies in cell dimensions can cause significant variation in ink transfer (Savickas et al., 2021; Bohan et al., 2001).

While previous studies have explored ink transfer characteristics and print quality at a broad level (Gencoglu, 2005; Deng et al., 2014), there remains a lack of systematic, quantitative investigations linking specific gravure engraving parameters to white ink consumption and spot color accuracy on transparent films. Research by Rich (2021) highlighted inconsistencies in the measurement of white ink contrast ratios due to variations in substrate reflectivity and instrument geometry, pointing to a need for standardized and replicable testing methods. Similarly, Eller and D'Amico (2022) and Chonillo and Eller (2024) demonstrated how changes in white ink coating weight significantly affect spot color fidelity,

yet they did not explore how cylinder geometry could be used as a controllable variable to optimize this relationship. Moreover, while studies like Chung and Hsu (2006) optimized process color gamut through ink sequence and engraving modifications, the evaluation of white inks and interactions with overlaid spot colors were minimally examined.

Current literature also lacks in-depth exploration of white ink behavior on modern transparent substrates such as CPET, with most prior work focusing on polyethylene terephthalate-glycol (PET-G), polyvinyl chloride (PVC) and Biaxially Oriented Polypropylene (BOPP) films (Joshi & Bandyopadhyay, 2015; Gencoglu, 2005). Research has yet to address how microstructural adjustments to cylinder engraving, through variables like stylus angle and screen angle can reduce white ink volume without degrading opacity or ΔE tolerances for overprinted chromatic inks. Additionally, although print mottle, gloss, and dot gain have been studied extensively (Valdec et al., 2017; Rong et al., 2004), few investigations link these surface phenomena to ink savings in the context of reverse-printed transparent packaging. This lack of exploration raises a fundamental research question: How do gravure cylinder engraving parameters affect white ink underlay and spot color reproduction on clear CPET films, and how can they be optimized to maintain quality while reducing ink consumption?

This study addresses these gaps by conducting a factorial experiment that analyzes how variations in gravure cylinder engraving parameters (line screen, screen angle, stylus angle) affect opacity, lightness and spot color fidelity (measured via ΔE00) when reverse-printed on clear CPET. This work investigates white ink performance as a foundational layer influencing overprinted spot colors. By identifying optimal combinations of cylinder engraving parameters that minimize white ink usage while maintaining acceptable spot color tolerances, this research provides both economic and environmental value.

Materials

In this experiment, solvent-based de-inkable gravure inks manufactured by a major ink supplier in North America were utilized, including a white ink formulation used as a backing in transparent substrates and two high-strength spot color inks corresponding to Pantone Matching Shade (PMS) 288 Blue and PMS 163 Orange. The formulated white ink was diluted using high-purity Ethyl Acetate 99.5% UG solvent, while the spot colors were adjusted using 3070 N-Propyl alcohol/acetate solvent blend. The test swatches were printed on a 45-micron clear CPET film. Printing trials were performed on an eight-stationed rotogravure printing press equipped with electromechanically engraved cylinders. All the printed samples were then evaluated using an X-Rite eXact Spectrodensitometer and ColorCert Suite software under D50/M0/2° measurement conditions. Statistical data analysis was performed using JMP Pro.

Methodology

To analyze the influence of engraving parameters and to identify optimal engraving combinations for reducing ink consumption, a full factorial design of experiments (DOE) was conducted described below. The DOE explored the relationship between engraving parameters in both single-hit and two-hit white underlay structures across multiple combinations of four-line screen levels, three screen angle levels and four stylus angle levels, when printed beneath the spot colors. Opacity and lightness (L*) were selected as primary dependent variables for the evaluation. Additionally, ΔE00 measurements were collected to assess spot color fidelity when printed over these white underlay configurations. Data collected from these measurements were analyzed and optimal combinations of engraving parameters were determined to minimize white ink usage while maintaining all the print parameters as per industry standards.

Experimental Design

For this research, test swatches were reverse printed according to a full factorial design of experiments. By combining multiple levels of line screen, screen angle, and stylus angle, white ink underlay was studied in two configurations: single-hit white ink underlay and a two-hit white ink underlay. The configurations were then reverse printed onto the substrate and measured for opacity and lightness against black backing. PMS 288 Blue and PMS 163 Orange were then overprinted on these underlayers to assess for ΔE00 measurements against the standard.

DOE Setup

A full factorial design of experiments (DOE) was initially developed to evaluate the effects of the examined combinations of the engraving parameters. The specific coded levels of each engraving parameter are summarized in Table 1.

Factors	Level 1	Level 2	Level 3	Level 4
Line Screen	2	3	4	5
Screen Angle	1	2	3	
Stylus Angle	1	2	3	4

Table 1: *Levels of each engraving parameters considered for the DOE*

The line screen represents the density of engraved cells on the cylinder surface, influencing ink laydown and resolution. The screen angle controls the orientation of the cell pattern affecting print smoothness and moiré visibility. The stylus angle influences cell depth and volume, impacting ink transfer efficiency and coverage.

Single-Hit Underlay DOE

A full factorial design for the single hit underlay structure, yielded 48 possible combinations (4 line screens × 3 screen angles × 4 stylus angles = 48), along with their cell volume (BCM) calculation.

Combinations with cell volume exceeding 12 BCM were eliminated due to their high volume of ink laydown. After filtering, 36 combinations were considered for engraving and testing (Outlined in Table A.2 of the Appendix).

Two-Hit Underlay DOE

For the two-hit underlay, a full factorial design was constructed by pairing two independent sets of engraving parameters (Set 1 and Set 2), which initially resulted in 2304 possible combinations (48 × 48 = 2304). Duplicate and symmetric combinations were removed. Cell volume was calculated for each combined set, and combinations with cell volume over 22 BCM were eliminated. After filtering, 677 unique combinations remained for further evaluation (outlined in Table A.4 of the Appendix).

Printing and Execution

A total of 24 printing trials were performed using gravure printing technique. Five cylinders were designed and engraved with coded combinations of the engraving parameters. The cylinders were used in various configurations to create combination swatches. Additionally, one cylinder was engraved to provide a flood coat layer of the spot color printed over the white swatches.

The press setup was optimized to minimize downtime between trials. Printing was performed at a constant press speed of 80 meters per minute. Swatches from Cylinders: Four and Five were printed first to form the bottom white layer, followed by swatches from Cylinders: One, Two, or Three forming the top white layer, with the spot color printed as the final (topmost) layer. The details of engraving combinations designed on each cylinder are provided in Appendix Table A.1.

For the first 12 trials, the white ink on all stations was diluted to a viscosity of 22 seconds using Zahn 2 cup. For the remaining 12 trials, the viscosity was adjusted to 19 seconds to study the influence of viscosity on ink laydown behavior. The spot color ink was maintained at 21 seconds viscosity throughout all trials. As viscosity is a critical parameter in gravure printing, ink viscosity at each station was monitored and manually adjusted every 20 minutes to ensure process consistency. The test prints were dried at 50°F through hot air dryers inbuilt at each station on the press.

Data Collection and Analysis

Cut sheets were extracted from each printed roll for measurement and analysis. Each test swatch was measured for print parameters mentioned in the Methodology section. Opacity and L* were measured using a Leneta Opacity Chart as the backing substrate, with L* specifically recorded against a black background to enhance differentiation of white ink coverage. The target reference standards were L* = 18.63, a* = 9.69, b* = -48.14 for PMS 288 Blue and L* = 75.26 a* = 28.86 b*= 36.89 for PMS 163 Orange. An average of three readings were taken per swatch to minimize measurement variability and improve data reliability. The detailed datasheet is available in Table A.3 and A.4 respectively, in the Appendix.

Correlation analysis was performed to evaluate the strength and directionality of relationships achieved between cell volume (BCM) and each print parameter. For opacity and lightness, one-way analysis of variance (ANOVA) was conducted to determine the statistical significance of BCM's influence on each variable. Additionally, linear regression models were developed to derive prediction equations. For spot color analysis, correlation analysis was proven sufficient.

The two-hit white underlay analysis aimed to identify optimal combinations of two different gravure cylinder engravings (BCM_1 and BCM_2 from Set 1 and Set 2) for achieving target print parameters while minimizing total ink consumption. Correlation analysis was performed to explore the relationships and two-way ANOVA models were constructed using BCM_1 and BCM_2 as continuous predictors to assess both their individual and interactive effects on output variables.

Optimization analysis was performed using the Prediction Profiler tool in JMP to identify the optimal engraving combinations for reducing ink consumption. Target criteria included opacity, L*values, ΔE00 values, and total BCM that were input into the model, while each parameter was also assigned weight based on its criticality. The tool simulated the effects of BCM_1 and BCM_2 on the key outputs, and combinations with the overall desirability score higher than the standard engraving set were selected as optimized combinations.

Results And Discussion

Results are presented for data collected with the single hit white underlay, followed by the two hit white underlay.

Single Hit White Underlay

Evaluation of the single hit white underlay presents opacity and lightness, followed by spot color evaluation.

Opacity and Lightness

In the single-hit white underlay, the relationship between the engraved cylinder's cell volume and both opacity and L* values were observed to be strong and positive. Higher BCM values led to increased opacity and L*, confirming that more ink laydown enhances visual whiteness, substrate masking, and perceived brightness. For example, engraving code 212[1] with 12 BCM achieved the highest opacity (54.2 at 22 seconds; 55.2 at 19 seconds) and L* value (73.57 at 22 seconds; 72.5 at 19 seconds), while code 534 with 3.5 BCM yielded the lowest opacity (38.3 at 22 seconds; 37.0 at 19 seconds) and L* (62.98 at 22 seconds; 61.91 at 19 seconds). The trend affirms the role of BCM as a dominant factor in controlling white ink optical performance.

Correlation Matrix	BCM	Opacity		Lightness	
		22 seconds	19 seconds	22 seconds	19 seconds
BCM	1.0000	0.9418	0.9789	0.9534	0.9613
Opacity (at 22 seconds)	0.9418	1.0000	0.9665	0.9810	0.9807
Opacity (at 19 seconds)	0.9789	0.9665	1.0000	0.9812	0.9889
Lightness (at 22 seconds)	0.9534	0.9810	0.9812	1.0000	0.9851
Lightness (at 19 seconds)	0.9613	0.9807	0.9889	0.9851	1.0000

Table 2: Correlations between BCM, Opacity and Lightness (L*) for single hit underlay

Engraving parameter combinations are represented in coded format to protect proprietary information shared by industry collaborators. Specific values for line screen, screen angle, and stylus angle have been anonymized in accordance with confidentiality agreements, while maintaining the integrity of experimental design and analysis.

Correlation analysis in Table 2 between the BCM and opacity was r = 0.9418 at 22 seconds viscosity and r = 0.9789 at 19 seconds ($p < 0.001$), while the correlation with L* was r = 0.9534 (22 seconds) and r = 0.9613 (19 seconds) ($p < 0.001$), all indicating very strong and statistically significant linear relationships. Although L* values were higher at 22 seconds viscosity, regression modeling revealed that 19 seconds viscosity allowed for comparable lightness and improved opacity using lower BCM values. The scatter plot matrix in Figure 1 further validates these trends, displaying tightly clustered, upward-sloping data with minimal variability, which supports the use of BCM as a reliable predictor for optimizing white ink underlay performance. Each scatter plot represents the relationship between two variables, where the x-axis indicates the predictor variable and the y-axis shows

the corresponding response. Individual dots represent measured data points, while the red regression line illustrates the linear fit across each relationship. Diagonal cells are labeled with the respective variable names, and the top-left corner of each scatterplot includes the Pearson correlation coefficient (r-value), quantifying the strength and direction of each association.

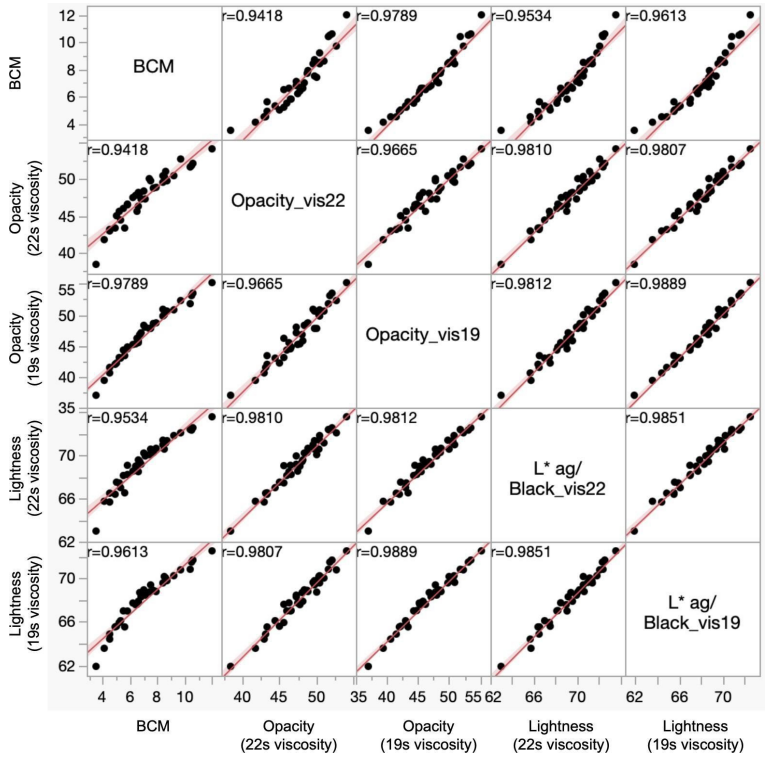


Figure 1: Scatter plot matrix of correlation between BCM, opacity and L* for single-hit white underlay

A one-way ANOVA confirmed the significance of cell BCM's influence on opacity under 19 seconds viscosity. The resulting regression model,

$$Opacity = 32.30 + 2.05 \times BCM1 \quad (1)$$

indicates that each unit increase in BCM results in an approximate 2.05-unit gain in opacity. The model was statistically significant ($F = 779.64$, $p < 0.0001$), and the lack-of-fit test was non-significant ($p = 0.1429$), validating the appropriateness of a linear model. Both the intercept and slope were statistically

significant ($p < 0.0001$). Figure 2 graphically represents the excellent model fit, with predicted opacity values at 19s viscosity closely matching actual observations ($R^2 = 0.9582$). The points closely aligned with the diagonal red line indicate a strong agreement between predicted and actual values.

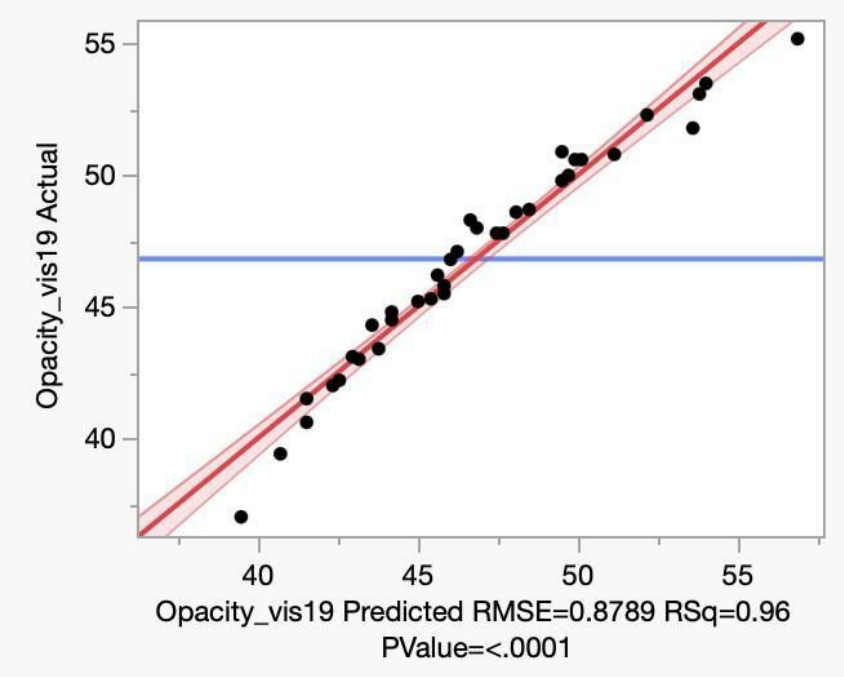


Figure 2: Actual vs. Predicted Opacity at 19s Viscosity

Based on the correlation strength, and regression performance, the 19 seconds viscosity condition was selected for further research and data collection. It provided higher opacity efficiency, supported brightness targets, and enabled potential white ink cost reduction.

Spot Color Fidelity

Spot Color Fidelity of the PMS 288 Blue and PMS 163 Orange over the white underlays at 19 seconds viscosity was evaluated using ΔE00, with a target of < 2.0 as per the industry practices. Across the dataset, ΔE00 values for PMS 288 Blue remained controlled, ranging from 0.11 (engraving set, coded 422) to 1.05 (engraving set, coded 212), indicating color stability. For PMS 163 Orange, ΔE00 values were higher, ranging from 1.41 to 2.21, with the highest occurring at the lowest BCM (engraving set, coded 534).

	BCM	ΔE00 PMS 288	ΔE00 PMS 163
BCM	1.0000	0.0353	-0.4586
ΔE00 PMS 288	0.0353	1.0000	0.1429
ΔE00 PMS 163	-0.4586	0.1429	1.0000

Table 3: Correlations between BCM and ΔE00 values for PMS 288 Blue and PMS 163 Orange

Table 3 shows the correlation analysis between engraving combination BCM and ΔE00 values for both spot colors. The correlation as observed was weak for PMS 288 Blue with r = 0.0353, suggesting that change in BCM had minimal influence on the color accuracy. Conversely, PMS 163 Orange showed a moderate negative correlation with r = -0.4586, indicating that increase in BCM resulted in lower ΔE00.

The scatterplot matrix in Figure 3 visually supported the correlation analysis by plotting pairwise relationships between BCM, ΔE00 (PMS 288), and ΔE00 (PMS 163). The BCM vs. ΔE00 PMS 288 plot showed a flat regression line and broadly scattered points, reinforcing the negligible correlation between these variables. In contrast, the BCM vs. ΔE00 PMS 163 plot revealed a downward-sloping regression line with a denser cluster of points, consistent with a moderate negative correlation and suggesting that increased ink laydown may lead to improved color fidelity for PMS 163. Additionally, the ΔE00 PMS 288 vs. ΔE00 PMS 163 scatter plot exhibits no distinct trend, visually affirming the weak relationship between the two spot colors' color deviations. The observed differences between PMS 163 Orange and PMS 288 Blue in their response to BCM variations can be attributed to their colorimetric properties. Warmer hues are more sensitive to substrate opacity and white underlay variability, making them more dependent on sufficient ink laydown for consistent reproduction. Color fidelity improvements need to be validated for a wider range of hues, particularly because different colors respond differently to underlay opacity, film transparency, and ink laydown variations in gravure printing. This suggests color dependent parameters for fidelity improvements: future researchers could examine a wider range of hues, particularly because different colors respond differently to underlay opacity, film transparency, and ink laydown variations in gravure printing. The entire data measured for opacity, L* and ΔE00 for all the engraving combinations for single hit white underlay is entailed in Table A.3 in the Appendix.

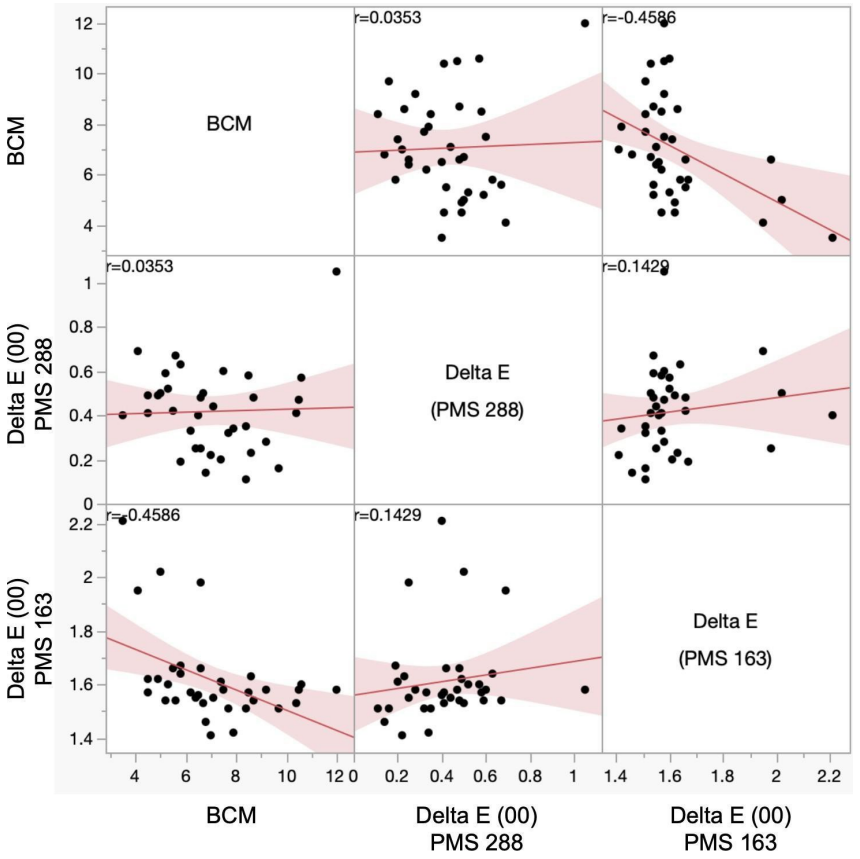


Figure 3: Scatter plot matrix of correlation between BCM and ΔE00 for single-hit white underlay

Two Hit White Underlay

Evaluation of the two-hit white underlay presents opacity and lightness, followed by spot color evaluation.

Opacity and Lightness

Within two-hit white underlay combinations, opacity ranged from 47.6 to 63.5, while L* values ranged from 69.14 to 77.99. The highest opacity was achieved with engraving code 213 in Set 1 and 212 in Set 2, both of which had high cell volume of 21.7 BCM. The lowest opacity was received on the combination 534 + 534, with the lowest cell volume of 7 BCM which indicated a direct correlation. The complete dataset for all two-layer engraving combinations, including

individual BCM_1, BCM_2, total BCM, and corresponding opacity and lightness values, is available in Appendix Table A.4.

Multivariate correlation analysis supported these findings with a strong positive relationship observed between cell volume i.e Total BCM ($BCM_1 + BCM_2$) and opacity ($r = 0.9560$), as well as L* ($r = 0.9632$), shown in Table 4.

	Total BCM	Opacity	Lightness	ΔE00 PMS 288	ΔE00 PMS 163
Total BCM	1.0000	0.956	0.9632	0.475	0.422
Opacity	0.956	1.0000	0.9715	0.4313	0.3996
Lightness	0.9632	0.9715	1.0000	0.4125	0.4235
ΔE00 PMS 288	0.475	0.4314	0.4125	1	0.3762
ΔE00 PMS 163	0.422	0.3996	0.4235	0.3762	1

Table 4: Correlations between BCM, Opacity, Lightness (L*) and ΔE00 for two-hit underlay

To further quantify these relationships, a two-way ANOVA was conducted with BCM_1 (bottom layer) and BCM_2 (top layer) as continuous predictors of printed opacity. The model demonstrated a strong fit ($R^2 = 0.9323$), with both BCM_1 and BCM_2 having statistically significant effects ($p < 0.0001$). The regression equation derived from the model:

$$Opacity = 43.96 + 1.076 \times BCM_1 + 0.965 \times BCM_2 \quad (2)$$

This result suggested that the first white hit (BCM_1) had more impact than the second layer. A similar two-way ANOVA was performed to evaluate the influence of BCM_1 and BCM_2 on L*. The model showed $R^2 = 0.9355$, and that both factors were again highly significant ($p < 0.0001$). The regression model for lightness:

$$L = 67.87 + 1.4116 \times BCM_1 + 0.5151 \times BCM_2 \quad (3)$$

The bottom-layer engraving (BCM_1) exerted a stronger influence on brightness than the top layer. These results suggested that optimizing the first white underlay is critical for improving both opacity and lightness.

The actual vs. predicted plots for both opacity and L* validate the reliability of the fitted regression models. As shown in Figure 4, the predicted values (x-axis) align closely with the actual measured values (y-axis), forming tight clusters around the red regression line with narrow confidence intervals. For opacity, the model yielded an R^2 of 0.92 and RMSE of 0.6959, while for L*, the model achieved an R^2 of 0.94 and RMSE of 0.3417, both with p-values < 0.0001. These metrics confirm that the model explains over 90% of the variance in the data and that BCM_1 and BCM_2 are strong predictors of both optical outcomes.

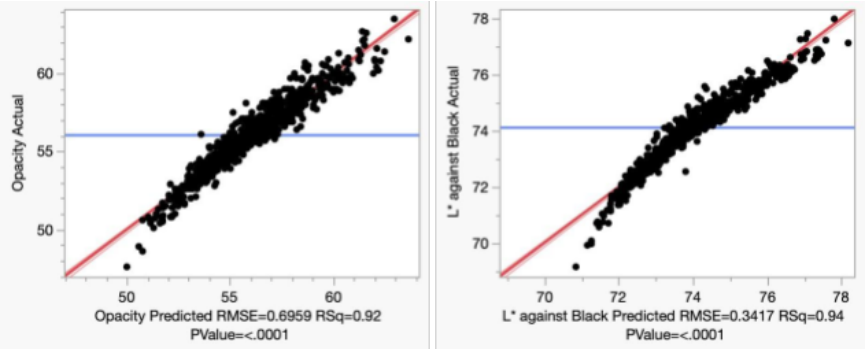


Figure 4: Actual vs. Predicted Opacity and Lightness (L*) for two-hit white underlay

Color Fidelity

All of the two-layer white ink configurations produced ΔE00 values below 2.0 for both PMS 288 Blue and PMS 163 Orange, indicating visually acceptable color fidelity across all combinations. To further understand the influence of engraving parameters on spot color accuracy, multivariate correlation analysis was performed between cell volume (Total BCM) and ΔE00 values. Moderate positive correlations were observed between cell volume and color deviation values. The correlation for PMS 288 Blue was r = 0.4750, while for PMS 163 Orange, r = 0.4220, indicated that higher white ink laydown was not directly associated with color deviation. However, the modest correlation strength indicated that factors beyond cell volume may also contribute significantly to color reproduction. The scatterplot matrix in Figure 5 visually confirmed the relationships among Total BCM, opacity, L*, and ΔE00 values for PMS 288 and PMS 163 under 19-second viscosity conditions. Strong upward-sloping clusters between Total BCM and both opacity and L* indicated a strong positive relationship, while the more dispersed clusters in the ΔE00 plots represented weaker correlations. These graphs justified the statistical interpretation that while optical density responded consistently to ink volume, color fidelity is less directly influenced by BCM alone.

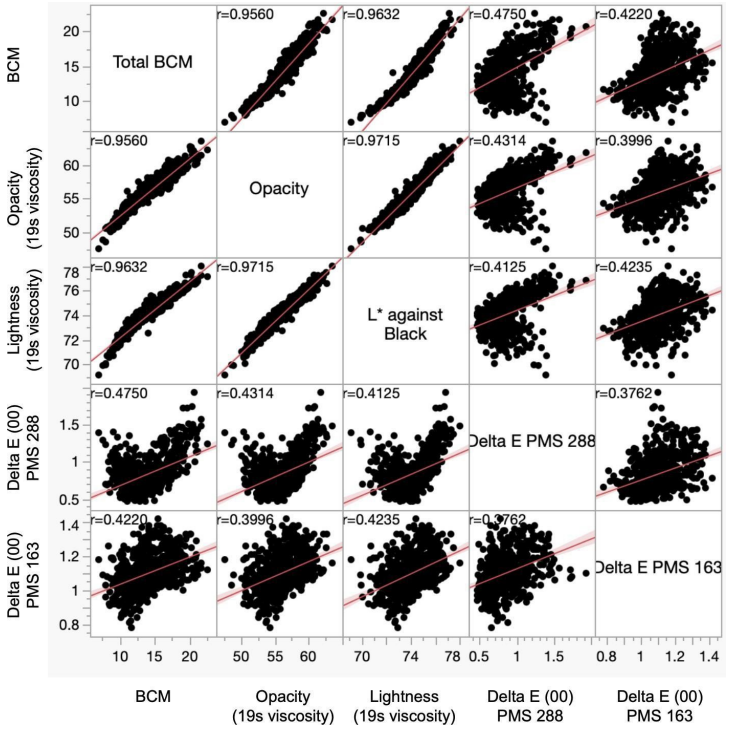


Figure 5: Scatter plot matrix of correlation between BCM and print parameters for two-hit underlay

For PMS 288 Blue, the regression model showed a relatively weak fit (R^2 = 0.2348), suggesting only ~23.5% of the ΔE00 variability can be explained by BCM_1 and BCM_2. However, both BCM_1 ($p < 0.0001$) and BCM_2 ($p < 0.0001$) had statistically significant effects. The regression equation derived was:

$$\Delta E00\ (PMS\ 288\ Blue) = 0.3146 + 0.0463 \times BCM_1 + 0.0277 \times BCM \qquad (4)$$

While statistically significant, the low R^2 implied that ΔE00 Blue was influenced more by factors outside of white ink underlay. Thus, BCM optimization alone was insufficient to control PMS 288 blue color accuracy in multi-layer gravure printing.

For PMS 163 Orange, the regression model also showed limited predictive power (R^2 = 0.2466). BCM_1 had a statistically significant effect ($p < 0.0001$), whereas BCM_2 did not ($p = 0.3354$). The fitted model achieved was:

$$\Delta E00\ (PMS\ 163) = 0.\ 897 + 0.\ 0256 \times BCM_1 + 0.\ 0020 \times BCM_2 \quad (5)$$

The coefficient for BCM_1 was positive but small, indicating that increased ink volume in the bottom layer might increase color deviation. However, the effect remained weak, and the top layer's contribution (BCM_2) remained negligible. The findings suggested that spot color fidelity for warmer hues like PMS 163 Orange was not improved through white underlay manipulation beyond a certain threshold.

The analyses reinforced that while two-hit white underlays could support acceptable color reproduction, achieving ΔE00 < 2 but also depended on the interplay of ink-substrate interactions.

Optimized Engraving Combinations

Optimization analysis was conducted using the Prediction Profiler tool in JMP, based on multivariate regression models incorporating BCM_1, BCM_2, and their interaction terms. These models enabled simulation of the impact of both engraving layers on the key parameters, facilitating optimization under the process constraints.

The following target criteria were defined, also represented in Figure 6:

- Opacity greater than 57, with a preferred range of 60–61
- Lightness (L*) value above 73
- ΔE00 < 2 for both PMS spot colors

Total BCM < 20.8, the benchmark set by the industry-standard engraving combination (312/312)

In the desirability setup, weights were assigned to each response variable, prioritizing opacity as the most critical output. Desirability scores ranged from 0 being least desirable to 1 being the most desirable, quantifying how well each parameter combination satisfies the defined targets. The curves in Figure 6 allows visual interpretation of how changes in BCM_1 and BCM_2 affect each output. For example, increasing BCM_1 steeply raised opacity and L*, while BCM_2 showed a smaller but still positive influence. However, both variables also slightly increased ΔE00 for PMS 288 and PMS 163, as seen in the upward trend of their response curves.

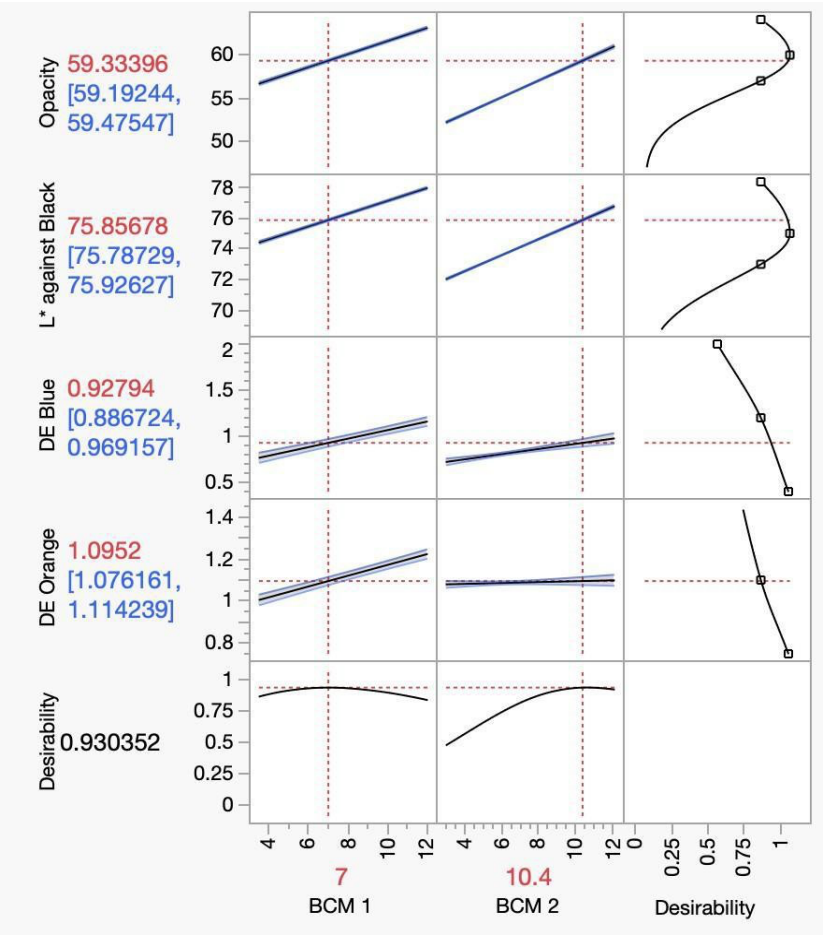


Figure 6: JMP Prediction Profiler showing optimal engraving performance with desirability score

A total of 33 engraving combinations outperformed the current industry standard, which comprised engraving code 312 for both layers (BCM total: 20.8). The optimized sets achieved total cell volume between 16.2 BCM and 19.7 BCM, indicating potential for reduction in ink consumption. Opacity values ranged from 58.6 to 61, and L* values exceeded 74 in all the optimized combinations. All combinations maintained ΔE00 below 2, demonstrating acceptable spot color fidelity. Among these configurations, the 323/312 (Set 1/Set 2) combination emerged as the most optimal, with 17.4 BCM and a desirability score of 0.93. Figure 6 represented the Prediction Profiler output from JMP showing the most optimized engraving combination (BCM_1 = 7, BCM_2 = 10.4) to achieve high opacity, lightness, and color fidelity with a desirability score. In comparison to

these optimized engraving combination sets, the current standard configuration (312/312) achieved a lower score of 0.88, showcasing the possibility of lesser ink consumption without compromising on print quality parameters. These optimized engraving combinations also offer flexibility depending on the desired balance between ink reduction, opacity enhancement, and color consistency. The full list of combinations with optimized performance metrics is provided in Appendix Table A.5 for consideration in future implementation.

Conclusion

The research examined the influence of gravure cylinder engraving parameters: line screen, screen angle, and stylus angle, on white ink underlay performance and spot color fidelity in reverse gravure printing on clear CPET film. Through a full factorial design of experiments, both single-hit and two-hit white underlays were analyzed under two distinct viscosity conditions (22 seconds and 19 seconds). The study aimed to optimize white ink consumption while maintaining critical visual and functional requirements, including opacity, lightness (L*), and spot color fidelity.

In the analysis for single-hit white underlay, strong positive correlations were observed between BCM and both opacity and lightness, with higher BCM producing brighter and more opaque prints. Regression and ANOVA analysis confirmed the statistical significance of these relationships. Color fidelity was controlled across all codes, with PMS 288 Blue, the ΔE00 values remaining largely unaffected by BCM, while PMS 163 Orange showed moderate sensitivity to change in white underlay structures, which also highlighted that color-specific characteristics interact with substrate and ink laydown behavior.

In the two-hit underlay configuration, the additive effect of BCM_1 and BCM_2 enhanced opacity and lightness. Statistical modeling revealed that both layers contribute significantly, with stronger influence of the first layer (BCM_1). While spot color fidelity for all combinations remained within acceptable thresholds ($\Delta E00 < 2$), multivariate correlation and ANOVA results indicated that factors beyond total BCM also play a crucial role in spot color accuracy. Particularly for PMS 288 Blue, BCM-based adjustments alone were insufficient to explain ΔE00 variation, whereas PMS 163 Orange showed more responsiveness to BCM_1 variations.

Optimization analysis demonstrated that high visual performance could be achieved with reduced ink laydown. A total of 33 optimized combinations were identified that met all quality constraints while reducing total BCM below the industry benchmark of 20.8. The most desirable configuration (323/312) achieved a desirability score of 0.93 with a total BCM of 17.4, thereby, delivering strong visual performance at a lower ink cost compared to the current standard (312/312, desirability 0.88). These optimized settings offer promising directions for

production implementation, enabling trade-offs between opacity, ink economy, and color consistency based on print requirements. Ultimately, this study validates the use of statistical design and multi-response optimization in gravure printing to advance both print quality and sustainability goals. Future work may explore broader color gamuts and process colors to further fine-tune the interplay between cylinder engraving parameters and ink performance.

References

Argent, D. (2008). *Opacity & White Ink*. Paper, Film & Foil Converter, https://www.pffc-online.com/print/inks/5759-opacity-white-ink-0101

Birchler, K. (n.d.). *Optimize Ink & Substrate*. Flexographic Technical Association, https://www.flexography.org/industry-news/optimize-ink-substrate/

Bohan, M., Clist, A. M., Claypole, T., & Gethin, D. T. (2001, January). Characterization of gravure cylinders. *Proceedings of the Technical Association of the Graphic Arts*.

Carpenter, L. (n.d.). *Optimizing White Ink for Flexibles* [Flexo Tech Talk]. Flexographic Technical Association, https://memberconnect.flexography.org/FTA/FLEXO_Magazine_Tech_Talks/Tech_Talks_2021-09-21.aspx?WebsiteKey=aa5ee36a-3256-4afe-8a68-9480a2663fcb b

Chen, S. H., Pua, S. T., Zhong, Z. W., & Shan, X. C. (2020). Investigation of Roll-to-Roll Gravure Printing for Printed Electronics with Fine Features. *Journal of Materials and Applications*, *9*(2), 79-89, https://www.xpublication.com/index.php/jma/article/view/458

Chonillo, J. X., & Eller, R. J. (2024, May 17). The relationship between white ink coating weight and color fidelity when blocking chromatic contents in compostable flexible packaging. *Journal of Print and Media Technology Research*, *13*(1), 7-16, https://jpmtr.org/index.php/journal/article/view/161

Chung, R. Y., & Hsu, F. (2006). Gravure Process Color Gamut Optimization. *Materials Science*, https://www.semanticscholar.org/paper/Gravure-Process-Color-Gamut-Optimization-Chung-Hsu/4be9de5333d85c06eff118a2fd6fd3ca5df7a512

Eller, R. J., & D'Amico, G. S. (2022, November 13). Characterizing the influence of white ink coating weight and print layer film type on chromaticity in gravure printed flexible packaging. *Journal of Print and Media Technology Research*, *11*(3), 183–193. https://www.jpmtr.org/index.php/journal/article/view/50

Gencoglu, E. N. (2005). The effects of some engraving and film substrate parameters on the solid density and the dot gain in gravure printing. *Surface Coatings International Part B Coatings Transactions*, *88*(1), 19-23. 10.1007/BF02699703

Joshi, A. V., & Bandyopadhyay, S. (2015). Effect of ink transfer on print mottle in shrink films. *Journal of Coatings Technology and Research*, *12*(1), 205-213, https://www.researchgate.net/publication/276317031_Effect_of_ink_transfer_on_print_mottle_in_shrink_films

Kumar, R., Chuhan, S., Kaushik, B., & Goyat, A. (2024, October 22). Comparative Analysis of Slur and Mottling on PP-White and PP-Clear Substrates in Flexographic Printing with UV-based Inks. *Nanotechnology Perceptions*, *20*(6), https://nano-ntp.com/index.php/nano/article/view/4264

Lloyd, S. (n.d.). *White Ink: The Most Critical Color To Control*. Flexographic Technical Association,

https://www.flexography.org/industry-news/white-ink-the-most-critical-color-to-control/

Martin, A. (2015). *Lab Colour Space and Delta E Measurements*. GRAPHIC DESIGN AND PRINT PRODUCTION FUNDAMENTALS, https://ecampusontario.pressbooks.pub/graphicdesign/chapter/4-4-lab-colour-space-and-delt a-e-measurements/

Neff, J. E. (2009, May 18). *Investigation of the effects of process parameters on performance of gravure printed ITO on flexible substrates*. George W. Woodruff School of Mechanical Engineering, https://repository.gatech.edu/entities/publication/4496c7e8-e20f-49f7-a533-a777fbcbdbb3

Ozcan, A., & Zulfigaroglu, R. (2020, December 1). An investigation on printability of different solvent based inks by gravure printing onto various substrates. *Journal of Graphic Engineering and Design*, *11*(2), 31–36, https://doi.org/10.24867/JGED-2020-2-031

Pu Jun, D., Wei, F., & Jian Dong, L. (2013, November). Study about Influencing of Printing Process on Gravure Printing Ink Transfer. *Applied Mechanics and Materials*, *469*, 301-304.10.4028, www.scientific.net/AMM.469.301

Renata, T., Dean, V., Mario, T., & Damir, V. (2023). The Impact of Underlying Opaque White Coating Parameters on Flexographic Print Quality. *Applied Sciences*, *13*(15), 857, https://doi.org/10.3390/app13158575

Rich, D. C. (2001). Consistent determination of the contrast ratio of white inks. *Journal of Coatings Technology and Research*, *18*(6), 1501-1509. 10.1007/s11998-021-00515-8

Rong, X., Pekarovic, J., & Pekarovicova, A. (2004). Gravure Printability From Laser and Electromechanically Engraved Cylinder. https://digitalcommons.calpoly.edu/grc_fac/20

Savickas, A., Stonkus, R., Jurkonis, E., & Iljin, I. (2021, October 27). Assessment of the Condition of Anilox Rollers. *Coatings*, *11*(11), 1301. https://doi.org/10.3390/coatings11111301

Sharma, B., Singh, S., Pandey, A., Dutt, D., & Kulshreshtha, A. (2023). Environment-friendly and cost-efective solution for fexible packaging printing process by advancement in engraving process. *Clean Technologies and Environmental Policy*, *25*, 909-920. https://doi.org/10.1007/s10098-022-02411-0

Sririnivasaraju, C. S. (2019, January 21). *A Comparison of Conventional and New Technology Gravure Cylinders in Terms of Image Quality*. Rochester Institute of Technology ProQuest Dissertations & Theses. https://www.proquest.com/docview/2300270702/9135FDB763654422PQ/1?accountid=108 &sourcetype=Dissertations%20&%20Theses

Valdec, D., Miljkovic, P., & Auguštin, B. (2017). The influence of printing substrate properties on color characterization in flexography according to the ISO specifications. *Technical Sciences*, *11*(3), 73-77. https://www.researchgate.net/publication/326541258_The_influence_of_printing_substrate_properties_on_color_characterization_in_flexography_according_to_the_ISO_specifications

Appendix

A.1: Cylinder Configurations

Appendix Table A.1 summarizes the engraving configurations used across all six gravure cylinders. Cylinders One through Three were engraved with 12 individual swatches each, measuring 98.5 mm × 100 mm. Cylinders Four and Five were engraved in a continuous band format measuring 130 mm × 5 mm, repeated 12 times around the cylinder circumference, with 18 distinct coded combinations engraved per cylinder. The banded layout enabled efficient sampling of multiple parameter sets within a single print run. Cylinder Six was engraved with a 940 mm × 250 mm flood coat area using a standard engraving configuration (312) and was used for the spot color overprint trials.

Cylinder No.	Swatch Format	Engraving Combinations Codes
Cylinder 1	98.5 mm × 100 mm	212, 312, 412, 512, 222, 322, 422, 522, 232, 332, 432, 532
Cylinder 2	98.5 mm × 100 mm	213, 313, 413, 513, 223, 323, 423, 523, 233, 333, 433, 533
Cylinder 3	98.5 mm × 100 mm	214, 314, 414, 514, 224, 324, 424, 524, 234, 334, 434, 534
Cylinder 4	130 mm × 5 mm, repeated 12 times	212, 222, 232, 312, 322, 332, 412, 422, 432, 512, 522, 532, 213, 223, 233, 313, 323, 333
Cylinder 5	130 mm × 5 mm, repeated 12 times	413, 423, 433, 513, 523, 533, 214, 224, 234, 314, 324, 334, 414, 424, 434, 514, 524, 534
Cylinder 6	940 mm × 250 mm, flood coat area	312 (standard engraving for spot color application)

A.2: Engraving Combinations used in DOE

Appendix Table A.2 lists the coded engraving parameter combinations used for single-hit and two hit white underlay configurations in the design of experiments (DOE). Each combination represents a set of line screen, screen angle, and stylus angle levels, along with the calculated cell volume expressed in billion cubic microns (BCM). These coded parameter sets were used to engrave individual single hit swatches that were used to print white layers in both single hit and two hit underlays.

Engraving Code	Line Screen	Screen Angle	Stylus Angle	BCM
212	2	1	2	12
213	2	1	3	9.7
214	2	1	4	7.5
222	2	2	2	10.6
223	2	2	3	8.6
224	2	2	4	6.7
232	2	3	2	10.5
233	2	3	3	8.5
234	2	3	4	6.6
312	3	1	2	10.4
313	3	1	3	8.4
314	3	1	4	6.6
322	3	2	2	8.7
323	3	2	3	7
324	3	2	4	5.5
332	3	3	2	8.4
333	3	3	3	6.8

334	3	3	4	5.3
412	4	1	2	9.2
413	4	1	3	7.4
414	4	1	4	5.8
422	4	2	2	7.1
423	4	2	3	5.8
424	4	2	4	4.5
432	4	3	2	7.7
433	4	3	3	6.2
434	4	3	4	4.9
512	5	1	2	7.9
513	5	1	3	6.4
514	5	1	4	5
522	5	2	2	6.5
523	5	2	3	5.2
524	5	2	4	4.1
532	5	3	2	5.6
533	5	3	3	4.5
534	5	3	4	3.5

A.3: Single Hit White Datasheet

Appendix Table A.3 presents the dataset generated from the single-hit white ink underlay experiments conducted as part of the DOE. Each row represents an engraving combination coded according to its specific line screen, screen angle, and stylus angle configuration. For each engraving code, the corresponding cell volume (BCM) value is listed, along with print parameter measurements recorded at two viscosity levels: 22 seconds and 19 seconds. The dataset captures how variations in cell volume and geometry impact white ink coverage and color reproduction. This table supports all correlation and ANOVA analyses referenced throughout the Results and Discussion section and forms the basis for determining the optimal balance between visual performance and ink consumption in gravure printing.

Code	BCM	Opacity		L* against black		ΔE00	
		Vis 22s	*Vis 19s*	*Vis 22s*	*Vis 19s*	*PMS 288*	*PMS 163*
212	12	54.2	55.2	73.57	72.5	1.05	1.58
213	9.7	52.8	52.3	72.08	70.76	0.48	1.54
214	7.5	49.8	47.8	70.57	69.38	0.23	1.63
222	10.6	52.2	53.5	72.55	71.66	0.57	1.6
223	8.6	51.1	50.6	71.15	70.01	0.44	1.55
224	6.7	48.1	46.8	69.42	68.68	0.2	1.61
232	10.5	51.9	53.1	72.33	71.47	0.47	1.58
233	8.5	50.4	50	70.57	70.15	0.32	1.51
234	6.6	46.3	45.5	68.48	67.74	0.19	1.67
312	10.4	51.7	51.8	72.39	70.81	0.41	1.53
313	8.4	50.5	49.8	71.4	69.56	0.34	1.42
314	6.6	48.2	45.8	69.57	67.88	0.33	1.57
322	8.7	49.8	50.6	71.36	69.77	0.28	1.58
323	7	48.4	48.3	70.21	68.93	0.22	1.41
324	5.5	46	44.3	68.13	67	0.48	1.66
332	8.4	49.6	50.9	70.98	69.61	0.4	1.56
333	6.8	47.3	47.1	69.17	68.29	0.14	1.46
334	5.3	44.4	43	67	66.1	0.42	1.66

412	9.2	50.5	50.8	71.83	70.22	0.35	1.51
413	7.4	50.1	47.8	70.06	68.72	0.58	1.57
414	5.8	46.5	44.5	69.07	66.99	0.6	1.58
422	7.1	47.3	48	69.94	68.44	0.11	1.51
423	5.8	46.6	44.8	68.22	67.03	0.5	1.53
424	4.5	43.1	41.5	66.49	64.87	0.49	1.62
432	7.7	48.8	48.6	70.27	68.88	0.16	1.51
433	6.2	47.5	45.2	68.53	67.72	0.41	1.57
434	4.9	43.3	42	66.39	65.53	0.49	1.62
512	7.9	48.9	48.7	70.65	68.77	0.67	1.54
513	6.4	47.8	45.3	68.99	67.57	0.59	1.54
514	5	45	42.2	67.51	65.59	0.63	1.64
522	6.5	45.6	46.2	69.04	67.6	0.25	1.55
523	5.2	45.6	43.1	67.44	65.93	0.52	1.6
524	4.1	41.7	39.4	65.74	63.57	0.69	1.95
532	5.6	43.3	43.4	66.52	65.53	0.25	1.98
533	4.5	42.9	40.6	65.67	64.41	0.5	2.02
534	3.5	38.3	37	62.98	61.91	0.4	2.21

A.4: Two-hit White Datasheet

Appendix Table A.4 summarizes the results for the two-layer white ink underlay configurations evaluated in this study. Each row lists a unique combination of engraving codes (Set 1 and Set 2), which represent the bottom and top white ink layers, respectively. The corresponding individual BCM values for each cylinder (BCM_1 and BCM_2) are shown, along with the calculated Total BCM that represents the overall ink laydown volume across both layers. The table further encompasses opacity, lightness (L*) measured against a black backing, and ΔE00 values for PMS 288 Blue and PMS 163 spot colors. These data were used to evaluate the influence of combined engraving strategies on optical coverage and color fidelity, and served as the foundation for the correlation, ANOVA, and multi-response optimization analyses described in the Results and Discussion section.

SET 2	BCM 1	BCM 2	Total BCM	Opacity	SET 1	Lightness	ΔE00	
							PMS 288	*PMS 163*
322	12	8.7	20.7	61.8	212	76.83	1.93	1.1
332	12	8.4	20.4	60.9	212	76.72	1.74	1.08
412	12	9.2	21.2	60.9	212	76.89	1.43	1.09
422	12	7.1	19.1	60	212	76.03	1.72	1.07
432	12	7.7	19.7	60.7	212	76.36	1.72	1.12
512	12	7.9	19.9	60.6	212	76.26	1.51	1.06
522	12	6.5	18.5	59.6	212	76.05	1.47	1.1
532	12	5.6	17.6	58.3	212	75.65	1.13	1.06
213	12	9.7	21.7	61.4	212	77.23	1.57	1.13
223	12	8.6	20.6	62.1	212	76.79	1.46	1.11
233	12	8.5	20.5	61.2	212	76.69	1.5	1.18
313	12	8.4	20.4	61.5	212	76.52	1.44	1.13
323	12	7	19	60.3	212	76.37	1.46	1.15
333	12	6.8	18.8	59.8	212	76.02	1.29	1.1
312	10.4	10.4	20.8	60	312	76.51	1	1.07
322	10.4	8.7	19.1	58.9	312	76.1	1.01	1
332	10.4	8.4	18.8	58.8	312	75.97	1.05	1.04
412	10.4	9.2	19.6	59.4	312	76.1	0.86	1.06

422	10.4	7.1	17.5	58.4	312	75.47	1.1	1.05
432	10.4	7.7	18.1	58.6	312	75.8	0.98	1.02
512	10.4	7.9	18.3	58.3	312	75.61	1	1.04
522	10.4	6.5	16.9	57.6	312	75.06	0.87	1.04
532	10.4	5.6	16	56.1	312	74.58	1.32	1.03
313	10.4	8.4	18.8	59	312	75.91	1.08	1.05
323	10.4	7	17.4	58	312	75.56	0.99	1.07
333	10.4	6.8	17.2	57.8	312	75.23	0.88	1.08
412	9.2	9.2	18.4	59	412	75.7	0.83	1.09
432	9.2	7.7	16.9	59	412	75.35	0.79	1.03
512	9.2	7.9	17.1	58.9	412	75.1	0.77	1.02
522	9.2	6.5	15.7	57.3	412	74.64	0.78	1.05
532	9.2	5.6	14.8	55.9	412	74.14	0.67	0.98
422	7.9	7.1	15	56.9	512	74.71	0.66	1.06
512	7.9	7.9	15.8	57.6	512	74.83	0.64	1.11
522	7.9	6.5	14.4	56.3	512	74.45	0.59	1.09
532	7.9	5.6	13.5	55.4	512	73.79	0.59	1.12
212	10.6	12	22.6	62.2	222	77.13	1.24	1.12
222	10.6	10.6	21.2	60.8	222	76.74	1.14	1.12
232	10.6	10.5	21.1	60.2	222	76.85	1.31	1.15
312	10.6	10.4	21	60.4	222	76.6	1.13	1.21
322	10.6	8.7	19.3	59.4	222	76.11	1.07	1.14
332	10.6	8.4	19	59	222	76.07	1.12	1.11
412	10.6	9.2	19.8	59.7	222	76.18	0.94	1.17
422	10.6	7.1	17.7	58.5	222	75.42	1.14	1.16
432	10.6	7.7	18.3	59	222	75.85	1.03	1.14
512	10.6	7.9	18.5	59.3	222	75.75	0.93	1.15
522	10.6	6.5	17.1	58.6	222	75.23	0.89	1.04
532	10.6	5.6	16.2	56.9	222	74.68	0.84	1.03
223	10.6	8.6	19.2	59.6	222	76.13	1.07	1.18

233	10.6	8.5	19.1	58.9	222	75.81	1.13	1.15
313	10.6	8.4	19	59	222	75.93	1.14	1.09
323	10.6	7	17.6	59	222	75.81	1.14	1.09
333	10.6	6.8	17.4	58.2	222	75.61	1.13	1.03
312	8.7	10.4	19.1	59.7	322	76.2	0.88	1.14
322	8.7	8.7	17.4	58.9	322	75.63	0.82	1.13
332	8.7	8.4	17.1	58.5	322	75.83	0.86	1.13
412	8.7	9.2	17.9	58.6	322	75.77	0.92	1.13
422	8.7	7.1	15.8	57.5	322	75	0.77	1.13
432	8.7	7.7	16.4	58	322	75.55	0.92	1.13
512	8.7	7.9	16.6	58.5	322	75.24	0.77	1.17
522	8.7	6.5	15.2	57.5	322	74.75	0.69	1.22
532	8.7	5.6	14.3	56.6	322	74.21	0.68	1.14
323	8.7	7	15.7	57.7	322	75.16	0.81	1.13
333	8.7	6.8	15.5	57.5	322	75.11	0.81	1.16
412	7.1	9.2	16.3	57.6	422	75.2	0.94	1.3
422	7.1	7.1	14.2	56.4	422	74.48	0.8	1.3
432	7.1	7.7	14.8	57.4	422	74.77	0.71	1.25
512	7.1	7.9	15	56.7	422	74.71	0.82	1.35
522	7.1	6.5	13.6	55.7	422	74.03	0.9	1.27
532	7.1	5.6	12.7	54.5	422	73.46	0.65	1.25
412	6.5	9.2	15.7	57.9	522	75.01	0.78	1.31
522	6.5	6.5	13	55.4	522	73.82	0.7	1.25
532	6.5	5.6	12.1	53	522	73.36	0.63	1.19
232	10.5	10.5	21	61.6	232	76.9	1.38	1.29
312	10.5	10.4	20.9	60.8	232	76.69	1.22	1.19
322	10.5	8.7	19.2	59.6	232	76.28	1.14	1.18
332	10.5	8.4	18.9	59.5	232	76.06	1.19	1.27
412	10.5	9.2	19.7	59.9	232	76.24	1.24	1.32
422	10.5	7.1	17.6	58.9	232	75.71	1.07	1.26

432	10.5	7.7	18.2	59.2	232	75.89	1.2	1.18
512	10.5	7.9	18.4	59.1	232	75.9	1.12	1.22
522	10.5	6.5	17	58.2	232	75.54	1.06	1.15
532	10.5	5.6	16.1	58.8	232	75.31	0.96	1.16
233	10.5	8.5	19	59.8	232	76.34	1.14	1.21
313	10.5	8.4	18.9	60.1	232	76.27	1.32	1.15
323	10.5	7	17.5	59.2	232	75.81	1.04	1.22
333	10.5	6.8	17.3	58.7	232	75.49	1.07	1.2
332	8.4	8.4	16.8	58	332	75.36	1.01	1.29
412	8.4	9.2	17.6	58.6	332	75.45	1.05	1.1
422	8.4	7.1	15.5	56.9	332	74.7	0.89	1.14
432	8.4	7.7	16.1	57.3	332	74.96	0.79	1.15
512	8.4	7.9	16.3	57.1	332	74.85	0.83	1.17
522	8.4	6.5	14.9	55.9	332	74.33	0.88	1.12
532	8.4	5.6	14	55.4	332	73.82	0.63	1.18
432	7.7	7.7	15.4	57.4	432	74.84	0.74	1.16
512	7.7	7.9	15.6	57.1	432	74.77	0.71	1.23
522	7.7	6.5	14.2	56.1	432	74.25	0.65	1.38
532	7.7	5.6	13.3	54.3	432	73.63	0.67	1.29
532	5.6	5.6	11.2	53.1	532	72.62	0.64	1.24
413	12	7.4	19.4	61.3	212	76.03	1.19	1.26
423	12	5.8	17.8	58.7	212	75.6	1.28	1.19
433	12	6.2	18.2	59.6	212	75.8	1.23	1.3
513	12	6.4	18.4	59.3	212	75.58	1.17	1.29
523	12	5.2	17.2	58.6	212	75.23	1.04	1.26
533	12	4.5	16.5	57.9	212	74.95	1.12	1.27
214	12	7.5	19.5	60	212	76.13	1.42	1.3
224	12	6.7	18.7	59.3	212	75.97	1.36	1.23
234	12	6.6	18.6	59.1	212	75.79	1.18	1.29
314	12	6.6	18.6	59.2	212	75.68	1.23	1.31

324	12	5.5	17.5	58.8	212	75.36	1.13	1.29
334	12	5.3	17.3	58.2	212	75.16	1	1.26
414	12	5.8	17.8	58.4	212	75.36	1.05	1.28
424	12	4.5	16.5	57.5	212	74.99	0.96	1.31
434	12	4.9	16.9	57.4	212	75.01	1.03	1.27
514	12	5	17	57.7	212	75.1	0.91	1.28
524	12	4.1	16.1	57	212	74.8	0.82	1.27
534	12	3.5	15.5	56.7	212	74.41	0.78	1.42
413	10.4	7.4	17.8	57.8	312	75.4	0.83	1.1
423	10.4	5.8	16.2	56.9	312	74.59	0.73	1.2
433	10.4	6.2	16.6	57.9	312	74.98	0.81	1.12
513	10.4	6.4	16.8	57.5	312	74.72	0.75	1.08
523	10.4	5.2	15.6	56.9	312	74.35	0.74	1.07
533	10.4	4.5	14.9	55.6	312	74.16	0.69	1.12
324	10.4	5.5	15.9	56.6	312	74.74	0.75	1.1
334	10.4	5.3	15.7	56.1	312	74.38	0.74	1.11
414	10.4	5.8	16.2	56.8	312	74.71	0.78	1.13
424	10.4	4.5	14.9	56.2	312	74.25	0.68	1.18
434	10.4	4.9	15.3	55.9	312	74.37	0.88	1.17
514	10.4	5	15.4	56.8	312	74.27	0.72	1.15
524	10.4	4.1	14.5	56.1	312	74.01	0.68	1.22
534	10.4	3.5	13.9	55.3	312	73.71	0.67	1.2
413	9.2	7.4	16.6	57.9	412	74.94	0.81	1.06
423	9.2	5.8	15	56.5	412	74.37	0.77	1.04
433	9.2	6.2	15.4	57.1	412	74.69	0.8	1.02
513	9.2	6.4	15.6	56.8	412	74.37	0.71	1.08
523	9.2	5.2	14.4	56.4	412	73.94	0.71	1.16
533	9.2	4.5	13.7	55	412	73.6	0.7	1.17
414	9.2	5.8	15	56.5	412	74.39	0.71	1.09
424	9.2	4.5	13.7	55.7	412	73.76	0.67	1.12

434	9.2	4.9	14.1	56.2	412	73.87	0.71	1.1
514	9.2	5	14.2	55.6	412	73.88	0.73	1.06
524	9.2	4.1	13.3	54.6	412	73.47	0.78	1.15
534	9.2	3.5	12.7	54.1	412	73.07	0.78	1.15
513	7.9	6.4	14.3	55.8	512	74.23	0.92	1.03
523	7.9	5.2	13.1	55	512	73.79	0.93	1.06
533	7.9	4.5	12.4	54.1	512	73.35	0.93	1.15
514	7.9	5	12.9	54.9	512	73.5	1.09	1.07
524	7.9	4.1	12	54.2	512	72.95	1.15	1.08
413	10.6	7.4	18	57.7	222	75.37	0.81	1.12
423	10.6	5.8	16.4	56.6	222	74.79	0.85	1.16
433	10.6	6.2	16.8	56.9	222	74.95	0.9	1.17
513	10.6	6.4	17	56.4	222	74.93	0.91	1.17
523	10.6	5.2	15.8	56	222	74.44	0.94	1.17
533	10.6	4.5	15.1	55.7	222	74.06	0.79	1.15
224	10.6	6.7	17.3	57.1	222	74.86	0.84	1.17
234	10.6	6.6	17.2	56.6	222	74.75	0.88	1.1
314	10.6	6.6	17.2	57.4	222	74.9	0.75	1.12
324	10.6	5.5	16.1	56.4	222	74.39	0.92	1.16
334	10.6	5.3	15.9	55.8	222	74.31	0.9	1.11
414	10.6	5.8	16.4	57	222	74.72	0.87	1.11
424	10.6	4.5	15.1	55.9	222	74.04	0.79	1.14
434	10.6	4.9	15.5	56.1	222	74.23	0.93	1.12
514	10.6	5	15.6	56.6	222	74.28	0.74	1.1
524	10.6	4.1	14.7	55.4	222	73.62	0.76	1.14
534	10.6	3.5	14.1	54.4	222	72.54	0.88	1.28
413	8.7	7.4	16.1	57.4	322	74.93	0.84	1.08
423	8.7	5.8	14.5	56.5	322	74.35	0.79	1.04
433	8.7	6.2	14.9	56.9	322	74.53	0.84	1.03
513	8.7	6.4	15.1	56.8	322	74.4	0.76	1.06

523	8.7	5.2	13.9	55.8	322	74.01	0.94	1.12
533	8.7	4.5	13.2	55.1	322	73.57	0.78	1.06
324	8.7	5.5	14.2	55.6	322	74.16	0.81	1
334	8.7	5.3	14	55.3	322	73.79	0.82	1.11
414	8.7	5.8	14.5	56.7	322	74.13	0.74	1.07
424	8.7	4.5	13.2	55	322	73.6	0.78	1.1
434	8.7	4.9	13.6	55.1	322	73.75	0.74	1.16
514	8.7	5	13.7	55.4	322	73.84	0.72	1.15
524	8.7	4.1	12.8	54.4	322	73.34	0.93	1.12
534	8.7	3.5	12.2	53.6	322	72.96	0.82	1.12
423	7.1	5.8	12.9	55.2	422	73.65	0.92	1.21
433	7.1	6.2	13.3	55.9	422	73.92	0.76	1.2
513	7.1	6.4	13.5	55.4	422	73.72	0.88	1.14
434	7.1	4.9	12	54	422	72.85	0.78	1.33
514	7.1	5	12.1	54.2	422	72.94	0.82	1.2
534	7.1	3.5	10.6	52.1	422	72.03	0.68	1.26
423	6.5	5.8	12.3	54.1	522	73.34	0.83	1.14
414	6.5	5.8	12.3	54.3	522	73.21	0.96	1.12
424	6.5	4.5	11	53.4	522	72.54	1.04	1.12
434	6.5	4.9	11.4	53.3	522	72.62	0.75	1.08
524	6.5	4.1	10.6	52.6	522	72.17	0.84	1.18
534	6.5	3.5	10	51.5	522	71.55	0.81	1.21
413	10.5	7.4	17.9	58.5	232	75.55	0.92	1.06
423	10.5	5.8	16.3	58.1	232	75.01	0.82	1.13
433	10.5	6.2	16.7	57.8	232	75.21	0.77	1.11
513	10.5	6.4	16.9	58.2	232	75.13	0.88	1.08
523	10.5	5.2	15.7	57.1	232	74.73	0.71	1.07
533	10.5	4.5	15	56.3	232	74.32	0.78	1.04
234	10.5	6.6	17.1	57.4	232	74.89	0.95	1.07
314	10.5	6.6	17.1	57.8	232	75.03	0.8	1.1

324	10.5	5.5	16	57	232	74.72	0.83	1.04
334	10.5	5.3	15.8	56.3	232	74.51	0.83	1.09
414	10.5	5.8	16.3	58.2	232	74.83	0.8	1.06
424	10.5	4.5	15	56.5	232	74.38	0.86	1.16
434	10.5	4.9	15.4	56.4	232	74.37	0.88	1.15
514	10.5	5	15.5	56.6	232	74.52	0.91	1.06
524	10.5	4.1	14.6	56.2	232	74.16	0.8	1.03
534	10.5	3.5	14	55.4	232	73.82	0.84	0.99
413	8.4	7.4	15.8	57.5	332	74.57	0.86	1.09
423	8.4	5.8	14.2	56.4	332	73.97	0.87	1.26
433	8.4	6.2	14.6	56.6	332	74.21	0.87	1.07
513	8.4	6.4	14.8	56.2	332	74.14	0.81	0.99
523	8.4	5.2	13.6	55.8	332	73.8	1.08	1.05
533	8.4	4.5	12.9	54.5	332	73.4	0.87	1.03
414	8.4	5.8	14.2	55.8	332	73.99	0.88	1.06
424	8.4	4.5	12.9	54.5	332	73.42	0.95	1.05
434	8.4	4.9	13.3	55.2	332	73.5	0.79	1.09
514	8.4	5	13.4	55.6	332	73.61	0.81	1.1
513	7.7	6.4	14.1	55.6	432	73.91	0.92	1.01
523	7.7	5.2	12.9	54.9	432	73.44	0.9	1.07
533	7.7	4.5	12.2	54.3	432	73.07	1.08	1.09
434	7.7	4.9	12.6	54.7	432	73.15	0.93	1.08
514	7.7	5	12.7	54.9	432	73.24	0.99	1.14
524	7.7	4.1	11.8	53.7	432	72.81	0.96	1.07
534	7.7	3.5	11.2	53	432	72.05	1.07	1.07
423	5.6	5.8	11.4	53.3	532	72.6	1.17	1.11
533	5.6	4.5	10.1	51.8	532	71.69	1.2	1.14
224	5.6	6.7	12.3	54.3	532	73.16	1.19	1.04
334	5.6	5.3	10.9	52.1	532	72.21	1.24	1.07
414	5.6	5.8	11.4	53	532	72.64	1.35	1.08

524	5.6	4.1	9.7	50.8	532	71.36	1.33	1.09
534	5.6	3.5	9.1	50.4	532	70.7	1.4	1.18
212	9.7	12	21.7	63.5	213	77.99	1.48	1.16
222	9.7	10.6	20.3	62.6	213	77.47	1.37	1.25
232	9.7	10.5	20.2	62.2	213	77.28	1.43	1.33
312	9.7	10.4	20.1	62.7	213	76.57	1.33	1.33
322	9.7	8.7	18.4	60.9	213	76.25	1.29	1.24
332	9.7	8.4	18.1	60.6	213	76.08	1.36	1.22
412	9.7	9.2	18.9	60.4	213	76.11	1.46	1.21
422	9.7	7.1	16.8	59.7	213	75.85	1.29	1.25
432	9.7	7.7	17.4	60.5	213	76.07	1.37	1.24
512	9.7	7.9	17.6	59.7	213	75.74	1.39	1.21
522	9.7	6.5	16.2	59	213	75.3	1.23	1.26
532	9.7	5.6	15.3	57.9	213	74.77	1.05	1.24
213	9.7	9.7	19.4	61	213	76.62	1.36	1.2
223	9.7	8.6	18.3	60.5	213	76.4	1.34	1.19
233	9.7	8.5	18.2	60.5	213	76.49	1.36	1.22
313	9.7	8.4	18.1	60	213	75.95	1.36	1.15
323	9.7	7	16.7	60	213	75.64	1.23	1.24
333	9.7	6.8	16.5	59.7	213	75.66	1.18	1.26
322	8.4	8.7	17.1	60.2	313	75.37	1.01	1.09
332	8.4	8.4	16.8	59.6	313	75.26	1	1.09
412	8.4	9.2	17.6	59.7	313	75.41	0.96	1.06
422	8.4	7.1	15.5	58	313	74.82	0.79	1.1
432	8.4	7.7	16.1	59	313	75.07	0.92	1.15
512	8.4	7.9	16.3	59	313	75.08	0.81	1.08
522	8.4	6.5	14.9	58.1	313	74.53	0.73	1.07
532	8.4	5.6	14	58.1	313	74.41	0.64	1.14
313	8.4	8.4	16.8	59.7	313	75.66	0.9	1.12
323	8.4	7	15.4	58.8	313	75.14	0.84	1.06

422	7.4	7.1	14.5	57.3	413	74.44	0.7	1.06
432	7.4	7.7	15.1	58.1	413	74.7	0.7	1.08
512	7.4	7.9	15.3	57.6	413	74.59	0.67	1.04
522	7.4	6.5	13.9	56.5	413	74.12	0.6	1.01
532	7.4	5.6	13	55.4	413	73.55	0.58	1.14
522	6.4	6.5	12.9	56.6	513	73.62	0.71	0.99
532	6.4	5.6	12	54.6	513	72.98	0.65	1.02
232	8.6	10.5	19.1	60.2	223	75.96	1.14	1.12
312	8.6	10.4	19	60.7	223	76.01	1.05	1.14
322	8.6	8.7	17.3	59.5	223	75.61	1.03	1.1
332	8.6	8.4	17	60.7	223	75.57	0.92	1.15
412	8.6	9.2	17.8	59	223	75.78	0.86	1.07
422	8.6	7.1	15.7	57.8	223	75.29	0.79	1.12
432	8.6	7.7	16.3	58.7	223	75.28	0.9	1.06
512	8.6	7.9	16.5	58.8	223	74.96	0.79	1.2
522	8.6	6.5	15.1	58.1	223	74.4	0.94	1.17
532	8.6	5.6	14.2	56.9	223	73.93	0.7	1.16
223	8.6	8.6	17.2	59.3	223	75.65	0.91	1.1
233	8.6	8.5	17.1	58.9	223	75.39	0.96	1.12
313	8.6	8.4	17	59	223	75.29	0.97	1.1
323	8.6	7	15.6	58.2	223	74.83	1	1.18
333	8.6	6.8	15.4	57.6	223	74.71	0.87	1.1
312	7	10.4	17.4	59	323	75.31	0.76	1.16
332	7	8.4	15.4	58.4	323	74.84	0.84	1.11
412	7	9.2	16.2	58.6	323	74.94	0.72	1.13
422	7	7.1	14.1	56.8	323	74.21	0.68	1.08
432	7	7.7	14.7	57.7	323	74.63	0.71	1.07
512	7	7.9	14.9	57.4	323	74.49	0.67	1.02
522	7	6.5	13.5	57.1	323	74.05	0.68	1.08
532	7	5.6	12.6	55.6	323	73.52	0.62	1.16

323	7	7	14	57.5	323	74.39	0.68	1.05
333	7	6.8	13.8	56.9	323	74.29	0.68	1.06
412	5.8	9.2	15	57.7	423	74.62	0.71	0.97
432	5.8	7.7	13.5	57.1	423	74.27	0.71	1.01
512	5.8	7.9	13.7	56.8	423	74.12	0.66	1.04
422	5.2	7.1	12.3	55.2	523	73.39	0.84	1.09
522	5.2	6.5	11.7	54.3	523	73.01	0.86	1.1
532	5.2	5.6	10.8	52.8	523	72.32	0.89	1.07
312	8.5	10.4	18.9	59.9	233	75.85	0.89	1.19
322	8.5	8.7	17.2	58.7	233	75.41	0.87	1.17
332	8.5	8.4	16.9	58.3	233	75.26	0.92	1.21
412	8.5	9.2	17.7	59.2	233	75.61	0.97	1.18
422	8.5	7.1	15.6	58	233	74.79	0.82	1.16
432	8.5	7.7	16.2	58.3	233	74.87	0.88	1.2
512	8.5	7.9	16.4	57.4	233	74.85	0.79	1.12
522	8.5	6.5	15	56.9	233	74.4	0.78	1.1
532	8.5	5.6	14.1	56.5	233	73.96	0.72	1.1
233	8.5	8.5	17	58.9	233	75.32	0.96	1.16
313	8.5	8.4	16.9	58.8	233	75.35	0.94	1.21
323	8.5	7	15.5	58.4	233	75.02	0.85	1.15
333	8.5	6.8	15.3	58.3	233	74.81	0.83	1.14
332	6.8	8.4	15.2	57.9	333	74.78	0.65	1.16
412	6.8	9.2	16	58.5	333	74.97	0.68	1.11
422	6.8	7.1	13.9	57.2	333	74.28	0.64	1.2
432	6.8	7.7	14.5	58.1	333	74.81	0.69	1.11
512	6.8	7.9	14.7	57.3	333	74.71	0.67	1.05
522	6.8	6.5	13.3	56.9	333	74.06	0.61	1.09
532	6.8	5.6	12.4	55.4	333	73.72	0.61	1.1
313	6.8	8.4	15.2	57.9	333	74.89	0.7	1.05
333	6.8	6.8	13.6	56.6	333	74.54	0.69	1.07

432	6.2	7.7	13.9	57.1	433	75.2	0.69	1.2
512	6.2	7.9	14.1	56.4	433	74.33	0.67	1.1
522	6.2	6.5	12.7	55.9	433	73.59	0.67	1.19
532	6.2	5.6	11.8	54.5	433	73	0.73	1.07
422	4.5	7.1	11.6	54.5	533	72.85	1.03	1.09
522	4.5	6.5	11	53.5	533	72.74	1	1.12
333	4.5	6.8	11.3	54.5	533	72.89	1.05	0.98
413	9.7	7.4	17.1	59.6	213	75.73	1.09	1.35
423	9.7	5.8	15.5	57.8	213	75.19	1.03	1.34
433	9.7	6.2	15.9	58.5	213	75.49	1.09	1.38
513	9.7	6.4	16.1	58.1	213	75.36	1.11	1.37
523	9.7	5.2	14.9	57.2	213	74.92	1.24	1.31
533	9.7	4.5	14.2	56.6	213	74.66	1.03	1.35
214	9.7	7.5	17.2	60.4	213	76.15	1.42	1.31
224	9.7	6.7	16.4	58.5	213	75.62	1.33	1.3
234	9.7	6.6	16.3	57.5	213	75.39	1.2	1.35
314	9.7	6.6	16.3	57.5	213	75.02	1.17	1.37
324	9.7	5.5	15.2	56.9	213	75	1.04	1.32
334	9.7	5.3	15	56.7	213	74.62	0.84	1.35
414	9.7	5.8	15.5	57.5	213	74.97	0.94	1.33
424	9.7	4.5	14.2	56.7	213	74.31	0.97	1.36
434	9.7	4.9	14.6	56.8	213	74.79	0.88	1.31
514	9.7	5	14.7	56.5	213	74.78	0.94	1.33
524	9.7	4.1	13.8	55.6	213	74.33	0.88	1.29
534	9.7	3.5	13.2	54.7	213	73.87	0.72	1.37
413	8.4	7.4	15.8	57.4	313	74.78	0.74	1.12
423	8.4	5.8	14.2	56	313	74.26	0.71	1.14
433	8.4	6.2	14.6	56.9	313	74.45	0.72	1.15
513	8.4	6.4	14.8	56.4	313	74.28	0.71	1.17
523	8.4	5.2	13.6	55.4	313	73.8	0.64	1.19

533	8.4	4.5	12.9	54.8	313	73.43	0.66	1.16
314	8.4	6.6	15	56.9	313	74.52	0.72	1.11
324	8.4	5.5	13.9	55.8	313	74.04	0.73	1.16
334	8.4	5.3	13.7	55.2	313	74.03	0.67	1.11
414	8.4	5.8	14.2	55.8	313	74.19	0.71	1.17
424	8.4	4.5	12.9	54.7	313	73.61	0.67	1.2
434	8.4	4.9	13.3	55.1	313	73.78	0.67	1.22
514	8.4	5	13.4	54.7	313	73.74	0.67	1.15
413	7.4	7.4	14.8	57.1	413	74.66	0.7	1.1
423	7.4	5.8	13.2	56.2	413	74.28	0.57	1.04
433	7.4	6.2	13.6	56.1	413	74.86	0.69	1.06
513	7.4	6.4	13.8	55.6	413	74.61	0.66	1.04
523	7.4	5.2	12.6	54.9	413	74.03	0.66	1.09
414	7.4	5.8	13.2	55.5	413	73.73	0.7	1.09
514	7.4	5	12.4	54.7	413	73.47	0.74	1.07
524	7.4	4.1	11.5	53.9	413	72.86	0.72	1.05
513	6.4	6.4	12.8	54.4	513	73.75	0.79	1.03
533	6.4	4.5	10.9	52.8	513	72.97	0.76	1.04
324	6.4	5.5	11.9	53.8	513	73.2	1.01	0.94
334	6.4	5.3	11.7	53.3	513	72.62	0.92	1.03
424	6.4	4.5	10.9	52.8	513	72.55	0.63	1.02
434	6.4	4.9	11.3	53.2	513	72.6	0.74	1.06
524	6.4	4.1	10.5	51.6	513	72.3	0.8	1.11
534	6.4	3.5	9.9	50.9	513	71.63	0.73	1.12
413	8.6	7.4	16	56.8	223	74.89	0.78	1.19
423	8.6	5.8	14.4	56.7	223	74.25	0.79	1.22
433	8.6	6.2	14.8	57.3	223	75.49	0.82	1.18
513	8.6	6.4	15	55.7	223	74.47	0.74	1.23
523	8.6	5.2	13.8	56	223	74.01	0.67	1.24
533	8.6	4.5	13.1	54.8	223	73.62	0.65	1.24

314	8.6	6.6	15.2	56.2	223	74.8	0.78	1.18
324	8.6	5.5	14.1	55.2	223	74.45	0.87	1.2
334	8.6	5.3	13.9	54.8	223	73.92	0.7	1.18
414	8.6	5.8	14.4	56.2	223	74.05	0.71	1.21
424	8.6	4.5	13.1	54.8	223	73.48	0.63	1.3
434	8.6	4.9	13.5	54.8	223	73.69	0.65	1.31
514	8.6	5	13.6	55	223	73.87	0.71	1.18
524	8.6	4.1	12.7	54.1	223	73.2	0.64	1.33
534	8.6	3.5	12.1	53.1	223	72.81	0.55	1.24
413	7	7.4	14.4	56	323	74.6	0.68	1.1
423	7	5.8	12.8	55.1	323	73.91	0.67	1.1
433	7	6.2	13.2	55.7	323	74.06	0.72	1.09
513	7	6.4	13.4	55.6	323	73.84	0.64	1.1
523	7	5.2	12.2	54.4	323	73.53	0.69	1.02
533	7	4.5	11.5	54.3	323	72.92	0.7	1.1
414	7	5.8	12.8	55.4	323	73.78	0.74	1.07
424	7	4.5	11.5	53.8	323	73.08	0.66	1.08
514	7	5	12	54	323	73.31	0.8	1.22
524	7	4.1	11.1	53.4	323	72.79	0.78	1.11
534	7	3.5	10.5	52	323	72.46	0.87	1.21
423	5.8	5.8	11.6	54.6	423	73.29	0.95	0.99
433	5.8	6.2	12	54.7	423	73.51	0.89	0.97
513	5.8	6.4	12.2	54.8	423	73.45	0.82	1.05
533	5.8	4.5	10.3	52.8	423	72.45	0.94	1.12
224	5.8	6.7	12.5	54.9	423	73.67	0.81	0.98
324	5.8	5.5	11.3	54	423	73.13	0.82	1.05
414	5.8	5.8	11.6	54.2	423	73.19	0.87	1.09
424	5.8	4.5	10.3	52.7	423	72.6	0.9	1.06
434	5.8	4.9	10.7	52.9	423	72.57	0.89	1.04
514	5.8	5	10.8	53	423	72.67	0.86	1.01

524	5.8	4.1	9.9	51	423	72.12	0.95	1.03
534	5.8	3.5	9.3	50.9	423	71.68	0.96	1.07
423	5.2	5.8	11	54.5	523	72.87	1.04	0.95
433	5.2	6.2	11.4	54.5	523	73.14	0.87	0.97
513	5.2	6.4	11.6	54.4	523	73.11	0.98	0.98
523	5.2	5.2	10.4	53.1	523	72.57	0.97	1.08
533	5.2	4.5	9.7	52.1	523	71.97	1.05	0.99
224	5.2	6.7	11.9	54.7	523	73.24	0.98	0.99
414	5.2	5.8	11	53.2	523	72.8	1.09	0.99
424	5.2	4.5	9.7	52.1	523	72.08	1.03	0.99
524	5.2	4.1	9.3	51.5	523	71.67	1.11	0.96
534	5.2	3.5	8.7	50.1	523	71.03	1.08	1.07
413	8.5	7.4	15.9	57.2	233	75.04	0.82	1.25
423	8.5	5.8	14.3	56.4	233	74.44	0.8	1.12
433	8.5	6.2	14.7	56.3	233	74.67	0.91	1.23
513	8.5	6.4	14.9	56.1	233	74.51	0.78	1.1
523	8.5	5.2	13.7	55.3	233	74.29	0.78	1.16
533	8.5	4.5	13	55.9	233	73.87	0.7	1.1
214	8.5	7.5	16	57.4	233	75	0.9	1.1
224	8.5	6.7	15.2	56.6	233	74.86	0.86	1.1
234	8.5	6.6	15.1	55.9	233	74.4	0.8	1.07
314	8.5	6.6	15.1	56.4	233	74.94	0.8	1.09
324	8.5	5.5	14	55.7	233	74.21	0.73	1.11
334	8.5	5.3	13.8	54.9	233	73.77	0.73	1.14
414	8.5	5.8	14.3	55.8	233	74.27	0.79	1.12
424	8.5	4.5	13	55.2	233	73.81	0.73	1.16
434	8.5	4.9	13.4	54.9	233	73.92	0.78	1.18
514	8.5	5	13.5	55.2	233	74.17	0.74	1.19
524	8.5	4.1	12.6	54.8	233	73.44	0.75	1.14
534	8.5	3.5	12	53.7	233	73	0.71	1.22

413	6.8	7.4	14.2	56.7	333	74.47	0.66	1
423	6.8	5.8	12.6	55.6	333	73.69	0.72	1.06
433	6.8	6.2	13	55.4	333	73.85	0.66	1.12
513	6.8	6.4	13.2	55.7	333	73.66	0.63	1.12
523	6.8	5.2	12	54.5	333	73.32	0.63	1.03
324	6.8	5.5	12.3	54.6	333	73.51	0.63	1.06
334	6.8	5.3	12.1	54	333	73.16	0.66	1.05
414	6.8	5.8	12.6	54.5	333	73.69	0.67	1.04
514	6.8	5	11.8	54.4	333	73.16	0.65	1.06
534	6.8	3.5	10.3	52.6	333	72.32	0.62	1.03
433	6.2	6.2	12.4	54.9	433	74.18	0.73	1.01
513	6.2	6.4	12.6	54.2	433	73.98	0.65	1
533	6.2	4.5	10.7	52.6	433	72.83	0.71	1.04
324	6.2	5.5	11.7	54	433	73.37	0.82	1.04
434	6.2	4.9	11.1	53.1	433	72.77	0.79	1.04
514	6.2	5	11.2	53.5	433	72.9	0.82	1.02
524	6.2	4.1	10.3	52.4	433	72.18	0.7	1.15
413	4.5	7.4	11.9	54.1	533	73.71	0.93	0.96
513	4.5	6.4	10.9	53.1	533	72.47	0.95	1
523	4.5	5.2	9.7	52	533	71.84	0.97	1.01
533	4.5	4.5	9	50.6	533	71.23	1.04	1.03
224	4.5	6.7	11.2	53.1	533	72.94	1	0.99
424	4.5	4.5	9	51.4	533	71.39	1.13	0.93
434	4.5	4.9	9.4	50.8	533	71.35	1.18	0.96
514	4.5	5	9.5	50.9	533	71.46	1.17	0.97
534	4.5	3.5	8	48.6	533	69.96	1.23	1.03
212	7.5	12	19.5	60.8	214	77.26	1.33	1.33
222	7.5	10.6	18.1	59.9	214	76.19	1.27	1.24
232	7.5	10.5	18	59.7	214	76.34	1.43	1.26
312	7.5	10.4	17.9	59.3	214	76.37	1.2	1.27

322	7.5	8.7	16.2	58.8	214	75.64	1.27	1.25
332	7.5	8.4	15.9	58.3	214	75.46	1.3	1.32
412	7.5	9.2	16.7	58.4	214	75.63	1.25	1.24
422	7.5	7.1	14.6	57.2	214	74.78	1.06	1.25
432	7.5	7.7	15.2	57.7	214	75.08	1.22	1.32
512	7.5	7.9	15.4	57.7	214	74.9	1.24	1.38
522	7.5	6.5	14	56.6	214	74.47	1.08	1.32
532	7.5	5.6	13.1	55.5	214	74.07	0.91	1.27
223	7.5	8.6	16.1	58.3	214	75.71	1.21	1.26
313	7.5	8.4	15.9	58.2	214	75.69	1.22	1.24
323	7.5	7	14.5	57.8	214	75.58	1.13	1.24
333	7.5	6.8	14.3	57.1	214	75.12	1.09	1.26
312	6.6	10.4	17	57.8	314	75.11	0.92	1.16
322	6.6	8.7	15.3	57.4	314	74.78	0.66	1.11
332	6.6	8.4	15	57	314	74.8	0.65	1.23
412	6.6	9.2	15.8	57	314	74.88	0.97	1.12
422	6.6	7.1	13.7	55.7	314	74.21	0.54	1.08
432	6.6	7.7	14.3	56.5	314	74.54	0.6	1.04
512	6.6	7.9	14.5	56.3	314	74.39	0.57	1.15
522	6.6	6.5	13.1	55.3	314	73.81	0.49	1.27
532	6.6	5.6	12.2	54	314	73.35	0.48	1.09
313	6.6	8.4	15	56.7	314	74.79	0.63	1.16
323	6.6	7	13.6	56.2	314	74.32	0.61	1.09
333	6.6	6.8	13.4	56	314	74.26	0.63	1.08
412	5.8	9.2	15	56.4	414	74.55	0.48	0.97
422	5.8	7.1	12.9	55.4	414	73.96	0.47	1
432	5.8	7.7	13.5	55.9	414	74.37	0.49	1.03
512	5.8	7.9	13.7	55.4	414	74.16	0.47	0.94
522	5	6.5	11.5	54.3	514	72.93	0.69	0.99
532	5	5.6	10.6	52.6	514	72.19	0.74	0.98

232	6.7	10.5	17.2	58.5	224	75.5	0.78	1.02
312	6.7	10.4	17.1	58.3	224	75.25	0.69	1.04
322	6.7	8.7	15.4	57.2	224	74.69	0.71	1.01
332	6.7	8.4	15.1	56.9	224	74.72	0.71	1.05
412	6.7	9.2	15.9	57.2	224	74.85	0.66	1.02
422	6.7	7.1	13.8	56	224	74.07	0.64	1.08
432	6.7	7.7	14.4	56.5	224	74.43	0.64	0.99
512	6.7	7.9	14.6	56.2	224	74.34	0.62	1.05
522	6.7	6.5	13.2	55.2	224	73.71	0.57	1.06
223	6.7	8.6	15.3	57.3	224	74.85	0.65	1.03
313	6.7	8.4	15.1	57.1	224	74.84	0.8	1.04
323	6.7	7	13.7	56.1	224	74.46	0.64	0.98
333	6.7	6.8	13.5	55.9	224	74.23	0.6	0.99
332	5.5	8.4	13.9	56.4	324	74.22	0.57	0.96
412	5.5	9.2	14.7	56.5	324	74.34	0.56	0.98
422	5.5	7.1	12.6	55.1	324	73.42	0.54	0.98
432	5.5	7.7	13.2	55.8	324	74.2	0.55	0.99
512	5.5	7.9	13.4	55.2	324	74.45	0.54	0.97
522	5.5	6.5	12	54.1	324	73.46	0.5	0.96
532	5.5	5.6	11.1	52.9	324	73.13	0.47	0.97
323	5.5	7	12.5	55.4	324	73.98	0.49	0.95
422	4.5	7.1	11.6	53.9	424	72.93	0.61	1.08
432	4.5	7.7	12.2	54.5	424	73.79	0.75	1.06
512	4.5	7.9	12.4	53.9	424	73.43	0.77	1.09
532	4.5	5.6	10.1	51.7	424	72.01	0.72	1.1
333	4.5	6.8	11.3	53.6	424	73.11	0.5	0.99
332	4.1	8.4	12.5	55.4	524	73.93	0.53	1
422	4.1	7.1	11.2	53.5	524	73.64	0.57	1.06
532	4.1	5.6	9.7	51.5	524	72.38	0.69	1.13
313	4.1	8.4	12.5	54.9	524	74.25	0.56	1.03

333	4.1	6.8	10.9	53.4	524	73.39	0.58	0.95
312	6.6	10.4	17	58	234	75.59	0.64	1.05
322	6.6	8.7	15.3	57.3	234	74.87	0.62	1.03
332	6.6	8.4	15	57.6	234	74.9	0.71	1.05
412	6.6	9.2	15.8	56.9	234	75	0.59	1.05
422	6.6	7.1	13.7	57	234	74.17	0.57	1.02
432	6.6	7.7	14.3	55.5	234	74.49	0.68	1.03
512	6.6	7.9	14.5	56.5	234	74.44	0.59	0.98
522	6.6	6.5	13.1	55	234	73.83	0.58	0.98
532	6.6	5.6	12.2	53.8	234	73.3	0.55	1.05
223	6.6	8.6	15.2	57.2	234	74.9	0.61	1.06
313	6.6	8.4	15	56.7	234	74.75	0.66	1.11
323	6.6	7	13.6	56.3	234	74.37	0.67	1.04
333	6.6	6.8	13.4	55.7	234	74.06	0.82	1.02
332	5.3	8.4	13.7	55.7	334	74.13	0.56	1.09
412	5.3	9.2	14.5	56.2	334	74.18	0.56	1.05
422	5.3	7.1	12.4	54.6	334	73.38	0.51	1.05
432	5.3	7.7	13	55.2	334	73.79	0.51	1.07
512	5.3	7.9	13.2	54.8	334	73.71	0.51	1.14
522	5.3	6.5	11.8	53.7	334	73.08	0.51	1.13
532	5.3	5.6	10.9	52.6	334	72.41	0.52	1.17
323	5.3	7	12.3	54.6	334	73.55	0.61	1.11
512	4.9	7.9	12.8	54.5	434	73.39	0.79	1.06
532	4.9	5.6	10.5	52	434	72.26	0.7	1.15
323	4.9	7	11.9	54.5	434	73.54	0.73	1.04
333	4.9	6.8	11.7	54.2	434	73.38	0.69	1.08
332	3.5	8.4	11.9	53.9	534	73.23	0.65	1.12
512	3.5	7.9	11.4	52.8	534	72.84	0.84	1.09
323	3.5	7	10.5	53.3	534	72.82	0.74	1.17
413	7.5	7.4	14.9	57.8	214	75.02	0.96	1.12

423	7.5	5.8	13.3	56.8	214	74.44	0.85	1.18
433	7.5	6.2	13.7	57.1	214	74.68	1.03	1.13
513	7.5	6.4	13.9	56.8	214	74.7	1.04	1.14
523	7.5	5.2	12.7	55.9	214	74.14	0.98	1.19
533	7.5	4.5	12	55.2	214	73.89	0.87	1.21
214	7.5	7.5	15	57.6	214	75.29	1.08	1.17
224	7.5	6.7	14.2	57.1	214	74.76	1.02	1.1
234	7.5	6.6	14.1	57.1	214	74.6	0.92	1.14
314	7.5	6.6	14.1	56.9	214	74.79	1.08	1.12
324	7.5	5.5	13	56.2	214	74.39	0.97	1.16
334	7.5	5.3	12.8	55.6	214	74.05	0.83	1.17
414	7.5	5.8	13.3	56	214	74.32	0.89	1.2
424	7.5	4.5	12	55.3	214	73.78	0.77	1.13
434	7.5	4.9	12.4	55.6	214	74.1	0.83	1.22
413	6.6	7.4	14	56.2	314	74.01	0.59	0.98
423	6.6	5.8	12.4	55.3	314	73.41	0.58	0.98
433	6.6	6.2	12.8	55.7	314	73.75	0.63	0.99
513	6.6	6.4	13	55.6	314	73.65	0.6	0.98
523	6.6	5.2	11.8	54.4	314	73.18	0.54	0.96
533	6.6	4.5	11.1	53.8	314	72.74	0.5	0.97
314	6.6	6.6	13.2	55.9	314	73.72	0.6	0.98
324	6.6	5.5	12.1	55.3	314	73.3	0.59	0.96
334	6.6	5.3	11.9	54.5	314	73.07	0.56	0.99
414	6.6	5.8	12.4	55.2	314	73.4	0.58	0.95
424	6.6	4.5	11.1	53.8	314	72.81	0.54	0.97
434	6.6	4.9	11.5	54.3	314	72.93	0.55	0.96
524	6.6	4.1	10.7	52.9	314	72.25	0.5	1.04
534	6.6	3.5	10.1	52.4	314	71.93	0.52	0.99
433	5.8	6.2	12	55.3	414	73.4	0.69	0.88
513	5.8	6.4	12.2	54.7	414	73.26	0.53	0.89

533	5.8	4.5	10.3	52.6	414	72.27	0.58	0.94
224	5.8	6.7	12.5	55.8	414	73.5	0.59	0.89
324	5.8	5.5	11.3	53.8	414	72.98	0.57	0.91
414	5.8	5.8	11.6	54.1	414	73.07	0.56	0.97
424	5.8	4.5	10.3	52.7	414	72.48	0.71	0.86
434	5.8	4.9	10.7	54.1	414	72.61	0.72	0.86
514	5.8	5	10.8	53.3	414	72.51	0.85	0.9
524	5.8	4.1	9.9	52.1	414	71.9	0.75	0.91
534	5.8	3.5	9.3	51.4	414	71.54	0.66	0.92
513	5	6.4	11.4	53.7	514	72.7	0.88	0.81
523	5	5.2	10.2	52.6	514	72.17	0.81	0.84
214	5	7.5	12.5	55.2	514	73.44	0.75	0.84
224	5	6.7	11.7	54.3	514	72.94	0.66	0.78
234	5	6.6	11.6	53.4	514	72.5	0.74	0.86
314	5	6.6	11.6	53.8	514	72.74	0.74	0.82
424	5	4.5	9.5	51.9	514	71.6	0.86	0.92
514	5	5	10	52.3	514	72.26	0.87	1.01
524	5	4.1	9.1	51.7	514	71.13	0.83	0.92
534	5	3.5	8.5	50.4	514	70.56	0.89	0.92
413	6.7	7.4	14.1	56.2	224	74.39	0.66	1.01
433	6.7	6.2	12.9	55.6	224	73.73	0.66	0.99
513	6.7	6.4	13.1	55.8	224	73.79	0.63	0.94
224	6.7	6.7	13.4	56.4	224	74.25	0.64	0.98
234	6.7	6.6	13.3	55.2	224	74	0.85	0.97
314	6.7	6.6	13.3	54.9	224	74.36	0.74	0.97
324	6.7	5.5	12.2	54.2	224	73.62	0.65	0.94
334	6.7	5.3	12	54.8	224	73.36	0.57	0.96
524	6.7	4.1	10.8	52.9	224	72.25	0.56	1.06
534	6.7	3.5	10.2	52.3	224	71.88	0.58	1.05
413	5.5	7.4	12.9	55.1	324	73.68	0.72	0.88

523	5.5	5.2	10.7	53.3	324	72.53	0.71	0.97
533	5.5	4.5	10	52.3	324	72.05	0.57	0.93
324	5.5	5.5	11	53.8	324	72.92	0.63	0.88
334	5.5	5.3	10.8	53	324	72.31	0.67	0.91
514	5.5	5	10.5	52.9	324	72.28	0.73	0.87
524	5.5	4.1	9.6	52.9	324	71.71	0.83	0.94
534	5.5	3.5	9	51.3	324	71.15	0.85	0.95
413	4.5	7.4	11.9	54.8	424	72.95	0.95	0.97
433	4.5	6.2	10.7	54.2	424	72.63	0.86	0.89
224	4.5	6.7	11.2	53.6	424	72.62	0.72	0.95
324	4.5	5.5	10	52.8	424	71.97	0.78	1.07
334	4.5	5.3	9.8	52.1	424	71.5	0.81	0.98
424	4.5	4.5	9	50.5	424	71.14	0.77	1.06
524	4.5	4.1	8.6	50.7	424	70.74	0.71	0.99
534	4.5	3.5	8	50.6	424	70.07	0.7	0.96
533	4.1	4.5	8.6	51	524	70.96	0.59	0.91
214	4.1	7.5	11.6	54.2	524	73.03	0.69	0.94
334	4.1	5.3	9.4	51.4	524	71.47	0.75	1.06
524	4.1	4.1	8.2	50.8	524	70.7	0.69	1.08
413	6.6	7.4	14	55.8	234	73.92	0.67	0.93
423	6.6	5.8	12.4	54.9	234	73.59	0.71	0.96
433	6.6	6.2	12.8	55.3	234	73.57	0.71	0.92
513	6.6	6.4	13	55.3	234	73.56	0.62	0.93
523	6.6	5.2	11.8	54.7	234	72.86	0.62	0.93
533	6.6	4.5	11.1	53.5	234	72.43	0.68	0.95
234	6.6	6.6	13.2	55.2	234	73.42	0.6	1.01
314	6.6	6.6	13.2	55.4	234	73.51	0.66	0.95
324	6.6	5.5	12.1	54.9	234	73.24	0.64	0.98
414	6.6	5.8	12.4	55.1	234	73.21	0.64	0.96
424	6.6	4.5	11.1	53.5	234	72.62	0.64	0.91

434	6.6	4.9	11.5	53.8	234	72.72	0.6	0.91
524	6.6	4.1	10.7	53.4	234	72.11	0.68	1.04
534	6.6	3.5	10.1	51.8	234	71.57	0.81	1.02
413	5.3	7.4	12.7	57.5	334	73.65	0.66	1.07
423	5.3	5.8	11.1	56.1	334	72.73	0.72	1.08
433	5.3	6.2	11.5	55.3	334	72.88	0.76	1.03
523	5.3	5.2	10.5	53.9	334	72.3	0.62	1.16
533	5.3	4.5	9.8	52.6	334	71.71	0.73	1.09
234	5.3	6.6	11.9	53.9	334	72.95	0.61	1.19
334	5.3	5.3	10.6	53.2	334	72.4	0.79	1.12
414	5.3	5.8	11.1	53.8	334	72.8	0.75	1.15
434	5.3	4.9	10.2	52.6	334	72.13	0.72	1.19
514	5.3	5	10.3	52.7	334	72.24	0.71	1.23
534	5.3	3.5	8.8	50.7	334	70.96	0.86	1.19
413	4.9	7.4	12.3	55.1	434	73.21	0.78	1.04
523	4.9	5.2	10.1	52.8	434	72.1	1.03	1.03
533	4.9	4.5	9.4	51.9	434	71.56	0.92	1.06
224	4.9	6.7	11.6	54.1	434	72.96	0.92	1.08
324	4.9	5.5	10.4	53.5	434	72.5	0.87	1.11
424	4.9	4.5	9.4	52.2	434	71.82	0.86	1.03
434	4.9	4.9	9.8	51.8	434	71.85	0.99	1.05
514	4.9	5	9.9	51.9	434	72.03	0.83	1.06
524	4.9	4.1	9	50.8	434	71.2	1	1.19
534	4.9	3.5	8.4	50.7	434	70.75	1	1.26
413	3.5	7.4	10.9	53.9	534	72.52	1.03	1.06
433	3.5	6.2	9.7	52	534	71.96	1.09	1.09
214	3.5	7.5	11	53.3	534	72.78	1.01	1.07
524	3.5	4.1	7.6	48.9	534	69.91	1.29	1.09
534	3.5	3.5	7	47.6	534	69.14	1.39	1.18

A.5: Optimized Engraving Combinations

Appendix Table A.5 lists the optimized engraving combinations identified through multi-response optimization using JMP's Prediction Profiler. Each combination that outperformed the current industry standard (312/312) by achieving higher overall desirability scores while maintaining target thresholds for opacity, lightness, ΔE00, and total BCM.

Performance	Set 1	Set 2	BCM 1	BCM 2	Total BCM	Opacity	Lightness	ΔE00 (PMS 288)	ΔE00 (PMS 163)	Desirability score
1	323	312	7	10.4	17.4	59	75.31	0.76	1.16	0.93
2	313	322	8.4	8.7	17.1	60.2	75.37	1.01	1.09	0.92
3	213	313	9.7	8.4	18.1	60	75.95	1.36	1.15	0.92
4	214	222	7.5	10.6	18.1	59.9	76.19	1.27	1.24	0.92
5	214	222	7.5	10.6	18.1	59.9	76.19	1.27	1.24	0.92
6	313	412	8.4	9.2	17.6	59.7	75.41	0.96	1.06	0.92
7	214	232	7.5	10.5	18	59.7	76.34	1.43	1.26	0.92
8	322	312	8.7	10.4	19.1	59.7	76.2	0.88	1.14	0.92
9	214	312	7.5	10.4	17.9	59.3	76.37	1.2	1.27	0.92
10	312	313	10.4	8.4	18.8	59	75.91	1.08	1.05	0.92
11	412	412	9.2	9.2	18.4	59	75.7	0.83	1.09	0.92
12	222	332	10.6	8.4	19	59	76.07	1.12	1.11	0.92
13	222	432	10.6	7.7	18.3	59	75.85	1.03	1.14	0.92
14	213	213	9.7	9.7	19.4	61	76.62	1.36	1.2	0.91
15	223	312	8.6	10.4	19	60.7	76.01	1.05	1.14	0.91
16	213	412	9.7	9.2	18.9	60.4	76.11	1.46	1.21	0.91
17	212	323	12	7	19	60.3	76.37	1.46	1.15	0.91
18	223	232	8.6	10.5	19.1	60.2	75.96	1.14	1.12	0.91
19	232	313	10.5	8.4	18.9	60.1	76.27	1.32	1.15	0.91
20	212	422	12	7.1	19.1	60	76.03	1.72	1.07	0.91
21	233	312	8.5	10.4	18.9	59.9	75.85	0.89	1.19	0.91
22	212	333	12	6.8	18.8	59.8	76.02	1.29	1.1	0.91

23	232	233	10.5	8.5	19	59.8	76.34	1.14	1.21	0.91
24	412	432	9.2	7.7	16.9	59	75.35	0.79	1.03	0.91
25	222	323	10.6	7	17.6	59	75.81	1.14	1.09	0.91
26	323	412	7	9.2	16.2	58.6	74.94	0.72	1.13	0.91
27	213	323	9.7	7	16.7	60	75.64	1.23	1.24	0.9
28	212	214	12	7.5	19.5	60	76.13	1.42	1.3	0.9
29	232	412	10.5	9.2	19.7	59.9	76.24	1.24	1.32	0.9
30	213	422	9.7	7.1	16.8	59.7	75.85	1.29	1.25	0.9
31	313	313	8.4	8.4	16.8	59.7	75.66	0.9	1.12	0.9
32	213	512	9.7	7.9	17.6	59.7	75.74	1.39	1.21	0.9
33	213	333	9.7	6.8	16.5	59.7	75.66	1.18	1.26	0.89
Std.	**312**	**312**	**10.4**	**10.4**	**20.8**	**60**	**76.51**	**1**	**1.07**	**0.88**